

Recent Advances in Self-Powered Electrochemical Biosensors for Early Diagnosis of Diseases

Vardan Galstyan,* Ilenia D'Onofrio, Aris Liboà, Giuseppe De Giorgio, Davide Vurro, Luigi Rovati, Giuseppe Tarabella, and Pasquale D'Angelo

Modern sensing technologies are highly required for health monitoring. In this respect, the development of small-size, high-performance, and self-powered biosensors for detecting and quantifying disease markers in biofluids can bring crucial changes and improvements to the concept of health monitoring systems. Clinical trials identify a wide range of biomarkers in biofluids that provide significant health information. Research into novel functional materials with outstanding properties opens up new perspectives for fabricating new-generation biosensors. Furthermore, energy conversion and storage units are investigated to integrate them into biosensors and develop self-powered systems. Electrochemical methods are very attractive for applications in biosensor technology, both in terms of biomarker detection and energy generation. Here the recent achievements in research into self-powered electrochemical biosensors to detect sweat and saliva biomarkers are presented. Potential biomarkers for efficient analysis of these fluids are discussed in light of their importance in identifying various diseases. The influence of electrode materials on the performance of sensors is discussed. Progress in developing operating strategies for self-powered electrochemical monitoring systems is also discussed. A summary and outlook are presented, mentioning major achievements and current issues to be explored.

1. Introduction

Modern requirements for personal healthcare have greatly increased the demand for developing sensing technologies with advanced functionalities. In contrast to conventional large-scale and costly diagnostic systems that require trained personnel, and laborious processes, new-generation sensing devices should be cost-effective, portable, and easy to use to perform real-time analysis. In this regard, developing biosensors for disease marker detection and quantification in biofluids indicates their great significance in biomedical diagnostics.^[1] In these devices, the biosignal is registered by the transducer, which converts it into a detectable output. The operating mechanism determines the output signal of biosensors.^[2] Electrochemical biosensors (ECBSs) convert bioreactive processes into electrical signals such as current, resistance, or potential changes.^[1d,3] In addition, the use of biological recognition elements

can significantly enhance their selectivity.^[1b,4] The advantages mentioned above as well as the relatively simple architecture and functionality of electrochemical biosensors make them suitable structures for the rapid detection of biomarkers in real time.

Conventional electrochemical sensors typically consist of three electrodes: working, reference, and counter. Heterogeneous reactions drive electrochemical sensing, where the working electrode and species in biofluids exchange charge carriers. Therefore, the electrode material plays a crucial role in these processes.^[3a] Research into exploring novel functional materials with attractive physicochemical properties opens up new perspectives for fabricating high-performance electrochemical biosensor systems and their application in human health monitoring. Furthermore, nanotechnology and nanoscale materials offer innovative tools to address issues associated with sensitivity, power consumption, and miniaturization of biosensors.^[1b,c,2c,5]

Typically, electrochemical sensors require an external power supply to operate, which is a problem in producing small portable or wearable sensors. Miniaturization of electrochemical sensors can reduce their power consumption. Furthermore, research shows that redox reactions using chemical species in biofluids generate energy that can be utilized to operate two-electrode

V. Galstyan, I. D'Onofrio, A. Liboà, G. De Giorgio, D. Vurro, G. Tarabella, P. D'Angelo

Institute of Materials for Electronics and Magnetism
National Research Council (IMEM-CNR)
Parco Area delle Scienze 37/A, Parma 43124, Italy
E-mail: vardan.galstyan@cnr.it

V. Galstyan, L. Rovati
Department of Engineering "Enzo Ferrari"
University of Modena and Reggio Emilia
Via Vivarelli 10, Modena 41125, Italy

I. D'Onofrio, A. Liboà
Department of Chemical
Life and Environmental Sustainability Sciences
University of Parma
P.co Area delle Scienze 11/a, Parma 43124, Italy

 The ORCID identification number(s) for the author(s) of this article can be found under <https://doi.org/10.1002/admt.202400395>

© 2024 The Author(s). Advanced Materials Technologies published by Wiley-VCH GmbH. This is an open access article under the terms of the [Creative Commons Attribution](https://creativecommons.org/licenses/by/4.0/) License, which permits use, distribution and reproduction in any medium, provided the original work is properly cited.

DOI: 10.1002/admt.202400395

electrochemical systems.^[3a,6] The power generated by electrochemical energy conversion varies depending on the concentration of the bioanalyte.^[3a,7] Thus, the above sensors can operate without an external power source. Various studies have reported the successful application of microbial fuel cells in self-powered biosensing, where one of the electrodes acts as an active sensing element.^[8] Using an electrochemical galvanic cell for biomarker detection is an efficient method for producing self-powered monitoring systems. Hence, an electrochemical sensor can function like a battery system, where the biofluids to be analyzed are also used as electrolytes and the redox reactions generate the electric current.^[9] Triboelectric nanogenerators can be used as an alternative strategy for developing self-powered biosensors.^[10] Here, mechanical energy is converted into electrical energy due to the electrification of the contact between a liquid and a solid,^[11] or the movement of a body.^[12]

The fabrication of new electrode structures with tunable adsorption and catalytic properties and the further development of effective strategies for electrochemical sensor architecture make them promising devices for detecting disease biomarkers in blood, sweat, and saliva.^[13] Progress in energy harvesting technologies that provide efficient solutions to increase energy output in electrochemical sensors is leading to the development of the next generation of health monitoring devices. Hence, evaluation of progress in self-powered ECBS research is necessary.

This paper discusses recent advances and current challenges in developing self-powered electrochemical sensors considering potential biomarkers for efficient analysis of blood, sweat, and saliva.

2. Biofluids and their Monitoring

Clinical studies have shown that biofluids such as blood, sweat, and saliva contain compounds that can be used as biomarkers for the early diagnosis of diseases. These findings encourage researchers to develop biosensor systems for rapid and real-time health monitoring. Recent advances in electrochemical biosensors make them very attractive for fabricating high-performance, self-powered monitoring devices to detect various biomarkers.

2.1. Monitoring of Blood

Blood is classified as a liquid connective tissue that performs many physiological functions due to its complex composition.^[14] It consists of corpuscular elements, i.e., red and white blood cells (erythrocytes and leukocytes, respectively) and platelets (thrombocytes). Cells or cell fragments are suspended in plasma, the liquid component of blood consisting mainly of water (90%). Plasma also contains various compounds, including proteins, electrolytes, carbohydrates, minerals, and fats.^[15] The transport of oxygen and nutrients to tissues and living cells is the main function of blood. However, it also serves a purification function by loading waste while releasing oxygen. Other important functions are delivering immune cells to areas where infections are present, buffering effect, and stabilizing body temperature.^[14] The highest levels of bioanalytes, present in other biometric indicators of the body, are characteristic of blood, therefore blood

test diagnostics can take advantage of this abundance. However, a major aspect makes it difficult to think of blood tests as a quick and cheap way to perform self-diagnostic tests. The complexity of whole blood is a limiting factor in making it the most suitable matrix for biosensor testing. In addition, the liquid components of blood, i.e., plasma, and serum, are also complex matrices, in which, first, many interfering molecules are similar to the selected analyte and can be detected. Various blood compounds may affect the activity of recognition elements. For instance, protein biofouling on the sensing interface in contact with the blood samples can cause a partial exposure of the active recognition interface to its conjugated analytes,^[16] while complex electrolytic environments in electrochemical biosensors may affect the biosensor performance.^[17]

2.1.1. Biomarkers in Blood

Various types of biomarkers can be measured in blood using a biosensor and can be used to detect and monitor several diseases. Intermediate or final metabolites play a fundamental role in human physiological activity. Detectable blood metabolites are typically small molecules with different functions and represent an important class of biomarkers for disease diagnosis (Figure 1). Main blood biomarkers and their threshold levels for the monitoring of diseases are reported in Table 1. The canonical example is glucose, one of the well-known molecules in the blood associated with health monitoring. From a physiological point of view, the maintenance of glucose concentration is tightly regulated.^[18] Excess glucose levels in the blood caused by metabolic disorders are harmful. Herein, diabetes mellitus is a major disease associated with excess glucose levels, causing several complications such as blindness, cardiovascular disease, and kidney failure.^[19] Expected normal glucose concentrations in blood range 70–100 mg dL⁻¹ (3.9–5.6 mmol L⁻¹). Glucose concentrations of 100–125 mg dL⁻¹ (5.6–6.9 mmol L⁻¹) are considered prediabetic, when the glucose level in the blood is higher than 126 mg dL⁻¹ (7 mmol L⁻¹), diabetes is diagnosed.^[20] Measuring glucose levels in this manner is critical for diagnosing and monitoring diabetes.

Another important metabolite associated with anaerobic glucose metabolism in muscle is lactate. When the level of lactate in the blood increases, a state of hyperlactatemia is achieved, which determines a decrease in pH. This condition results from tissue hypoperfusion and hypoxia occurring in shock, severe anemia, respiratory failure, and hypermetabolic states. However, it may also result from exposure to various drugs, toxins, mitochondrial defects, or sepsis that impair aerobic energy production and lactate consumption.^[21] A decrease in cellular pH can lead to cellular acidosis, which impairs muscle function.^[22] In a physiological scenario, whole lactate production levels range from 15 to 30 mmol kg⁻¹ day⁻¹. Normally, lactate concentration in the bloodstream is maintained at 0.5–1.0 mmol L⁻¹ due to a tightly regulated balance between lactate production and consumption. When lactate levels exceed 1.0 mmol L⁻¹ hyperlactatemia occurs.^[21] For these reasons, measuring blood lactate levels can provide important information for assessing disease severity or monitoring the health status of patients.

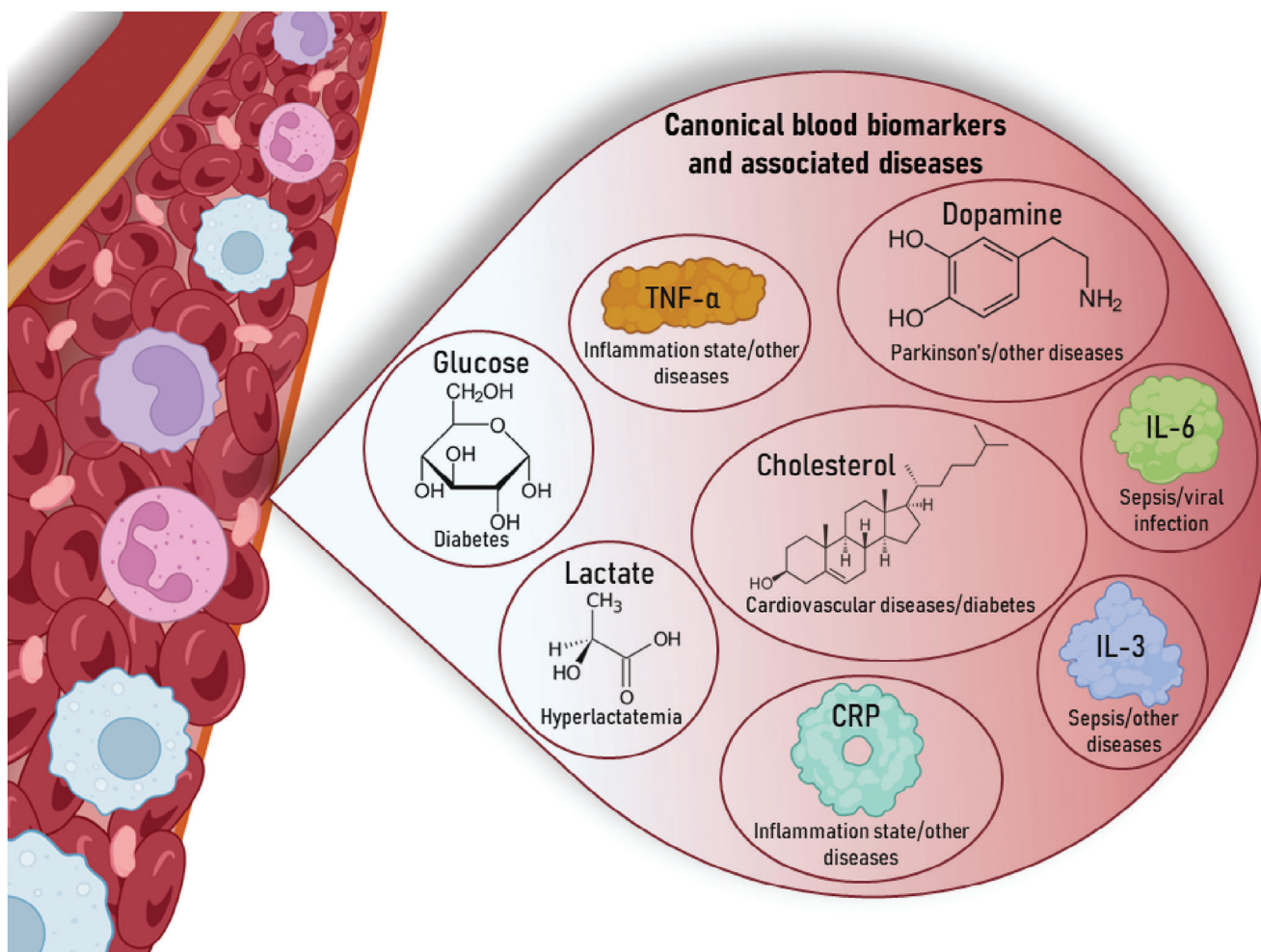


Figure 1. Schematic representation of some canonical blood biomarkers and their associated diseases. The range of components in human blood and its physiological functions make it rich in many biological data. Several markers in the blood are associated with the monitoring and diagnosis of many diseases. The markers presented in the schematic illustrate some recognition elements, the detection of which is important for the development of sensor systems for rapid health monitoring in real-time. Created with BioRender.com.

Table 1. Main blood biomarkers and their physiological concentration in blood. The onset of related diseases is associated with exceeding maximum concentration.

Biomarker	Concentration	Disease	Refs.
Glucose	70–126 mg dL ⁻¹	Diabetes	[20]
Lactate	0.5–1.0 mmol L ⁻¹	Hyperlactatemia	[21]
Cholesterol	200–250 mg dL ⁻¹	Cardiovascular diseases – diabetes	[23]
Dopamine	0.01–1 μM	Parkinson's disease – attention deficit hyperactivity disorder or other diseases	[27b]
CRP	0.02–13.5 mg L ⁻¹	Inflammation state or other diseases	[28a]
IL-3	> 89.4 pg mL ⁻¹	High mortality rate in sepsis or other diseases	[29a]
IL-6	>52.60 pg mL ⁻¹	Sepsis	[32]
IL-6	0–43.5 pg mL ⁻¹	COVID-19 or viral infection state	[33]
TNF-α	3.9–18.5 ng L ⁻¹	Inflammation state or other diseases	[35a]
Trysoin	> 1,4 μg mL ⁻¹	Pancreatic diseases	[36]

Cholesterol is an essential lipid, a component of cell membranes, and a common precursor for the biosynthesis of vitamin D, hormones, and bile acids. Genetic modification or increased intake of dietary lipids may upset the balance of blood cholesterol levels.^[23] In a healthy person, the blood cholesterol concentration should be below 200 mg dL⁻¹, and levels between 200 and 249 mg dL⁻¹ are considered borderline. A cholesterol level above 250 mg dL⁻¹ indicates several conditions (e.g., high blood pressure, heart attack, peripheral artery disease, stroke, and type 2 diabetes).^[23–24] Rapid and easy monitoring of blood cholesterol using biosensors is an important tool for assessing the risk of cardiovascular disease or other forms of disease associated with high cholesterol.

Neurotransmitters are endogenous messengers that transmit information between neurons and are represented by chemical substances that play an important role in the nervous system of the human body.^[25] Measuring levels of neurotransmitters in the blood can be important for monitoring health and detecting disease. Dopamine is an example of one of the most important and studied neurotransmitters, occupying a fundamental position in the central nervous system (CNS), binding to specific receptors on neuronal membranes, and playing a crucial role in the control of movement, learning, working memory, cognition, and emotion.^[26] Physiological levels of dopamine in the blood range from 0.01 to 1 μM. Dysregulation of dopamine levels underlies euphoria, attention deficit hyperactivity disorder, and Parkinson's disease. There is also growing evidence of dopamine hyperactivity in schizophrenia.^[27] Therefore, accurately determining dopamine levels is important for the early detection of these diseases.

One of the most important classes of biomarkers for recognizing diverse physiological blood parameters is represented by proteins. These biological macromolecules which provide a wide range of bodily functions, are useful for detecting and monitoring various blood biomarkers originating from multiple body tissues. The importance of proteins as biomarkers is also reflected in several diseases that can be detected or monitored. Herein, we will give examples of some of the most well-known protein biomarkers, in particular cytokines.

C-reactive protein (CRP) is a common blood biomarker. It is a pentameric protein synthesized by the liver and belongs to the class of opsonins. In the inflammatory state, CRP opsonizes the surface of microbes and dead or irreparably damaged cells, acting as an attack complex for complement proteins and promoting macrophage-mediated phagocytosis. Its level in healthy people is 0.02–13.5 mg L⁻¹, which may increase by four orders of magnitude due to inflammation or other disorders. Significant concentration fluctuations make the detection and monitoring of CRP a powerful tool for assessing the effectiveness of therapy and monitoring the progression of various diseases.^[28]

Interleukin-3 (IL-3) is an important blood biomarker for identifying inflammatory conditions and/or sepsis. It is an inflammatory cytokine that biologically promotes the production, proliferation, and survival of white blood cells. On the other hand, IL-3 enhances immune responses in sepsis, where high concentrations of IL-3 correlate with increased mortality. Infected patients with serum concentrations of >89.4 pg mL⁻¹ are associated with higher mortality rates.^[29] Therefore, blood IL-3 determination and monitoring are critical in some clinical circumstances.

Another pleiotropic cytokine is Interleukin 6 (IL-6), which plays a key role in host defense mechanisms. IL-6 is readily produced during inflammation, tissue damage, or infection, contributing to physiological acute phase immune responses, as well as hematopoiesis. Abnormal IL-6 levels are involved in different pathologies such as cancer, rheumatoid arthritis, autoimmune and chronic inflammatory diseases.^[30] IL-6 is recognized as an important biomarker for monitoring the acute phase of sepsis and is also considered a biomarker for cancer patients.^[31] The threshold level of IL-6 in the blood for diagnosing sepsis in healthy people is 52.60 pg mL⁻¹.^[32] The detection and monitoring of IL-6 was also evaluated in viral infections, including COVID-19, with blood levels in healthy donors ranging from 0 to 43.5 pg mL⁻¹, with higher concentrations associated with the infection state.^[33]

Another potent proinflammatory and immunoregulatory cytokine present in the blood corresponds to tumor necrosis factor (TNF) α , produced by tumor cells, fibroblasts, keratinocytes, macrophages, neutrophils, B, T, and NK cells, T and B cells.^[34] TNF α is a major mediator of the inflammatory and immune response in many pathologies such as cancer, multiple sclerosis, Parkinson's disease, inflammatory bowel disease, rheumatoid arthritis, and HIV.^[35] Thus, detection and monitoring of TNF- α levels in the blood is fundamental for the assessment of various diseases. The level of TNF- α in the blood in healthy people is 3.9–18.5 ng L⁻¹, higher concentrations are associated with inflammation and/or various pathologies.^[35b] Trypsin is a protein produced by the pancreas that is an important biomarker found in blood and serum. It plays a crucial role in diagnosing pancreatic diseases such as pancreatitis. Normal levels of trypsin in the blood are in the microgram range (0.25 mcg mL⁻¹). However, an acute pancreatic attack is indicated by a significant increase in trypsin concentration exceeding 1.4 μg mL⁻¹.^[36]

2.1.2. Detection of Biomarkers in Blood

Technological advances over the past decade in microfluidics, the fabrication of electrochemical biosensors, and diagnostic systems for biofluid examination, may offer advantages in diagnostics by allowing direct blood analysis. Biosensors, in particular, exploit recognition elements such as physiologically produced enzymes and antibodies, or even synthetic complex molecules such as aptamers and nanobodies, to accomplish their operation.^[37] This is independent of the transduction mechanisms they rely on.

The scientific literature of the sector demonstrates that it is quite challenging to find electrical and optical biosensors that are effective in testing whole blood. Indeed, the tendency to saturate the biosensor response due to analytes abundance in blood and interfering effects influencing the recognition efficiency mirrors the complexity of blood and related matrices. Preziosi et al. studied the response of organic electrochemical transistors (OECTs) in the presence of whole blood and plasma. Inter alia, they showed that, even in the case of OECTs gated by gold (Au) electrodes, which are less effective in promoting a channel current change in the presence of electrolytes, an almost undistinguishable response may be found by comparing whole blood and plasma responses.^[38] Indeed, Olkhov et al. have shown that a

Table 2. Parameters of ECBSs for the detection of biomarkers in blood and serum.

Anode material	Cathode material	Biomarker	Concentration/detection range	Output	LOD	Detection method	Refs.
Carbon Paper /FeMe ₂ -LPEI/GOx	Carbon Paper/ AnMWCNTs/Laccase	Glucose	1–20 mM	Power 0.19 μWn M ⁻¹	480 μM	Linear polarization	[42]
poly-methylene blue/ FAD-Glucose dehydrogenase (FADGDH) from <i>Aspergillus niger</i>	Bilirubin oxidase	Glucose	0,03–10 mM	Power 1.4 μW cm ⁻²	NA	Dependence between analyte concentration and power density	[43]
Silver/carbon ink/ FADGDH	BOx	Glucose	5–30 mM	NA	NA	Chronoamperometric measurement	[44]
MWCNT/NQ-LPEI/FAD-GDH	Silver oxide/carbon paste	Glucose	5–18 mM	Voltage 11.3 mV mM ⁻¹	NA	Charge of a capacitor	[13a]
PANI/TPU/GOx	PANI/TPU/	Glucose	5–10 mM	NA	NA	Dependence between the output current and glucose concentration	[45]
GOx- polyethyleneimine modified TCP	anthracene-modified MWCNTs laccase	Glucose	1–10 mM	Current 1.24 μA mM ⁻¹	0.48 mM	Dependence of generated energy and glucose concentration	[46]
Platinum-iridium wire /carbon black/vitamin K3/ Dp and GHD enzymes	carbon/BOD	Glucose	From 500 μmol L ⁻¹ to 100 mmol L ⁻¹	NA	NA	Dependence between glucose concentration and LED switch on	[47]
The sol-gel membrane of phenothiazine /ChOx	Carbon/Prussian blue/ChOx	Cholesterol	0.15 mmol L ⁻¹ to 4.1 mmol L ⁻¹	Current 26 mAmol Lcm ⁻²	1.4 μmol L ⁻¹	Dependence between output current and cholesterol concentration	[48]
NA	NA	Thrombin	From 3 nmol L ⁻¹ to 1.35 μmol L ⁻¹	NA	0.9 nmol L ⁻¹	Amperometric detection	[49]
Au/Mg/Al/WPI	Au	Trypsin	0,5 to 100 μg mL ⁻¹	NA	0.5 μg mL ⁻¹	Dependence between trypsin concentration and LED switch meantime	[50]

NA: Not available

tricky experimental method is needed to reduce the sources of interference in optical biosensors, such as light absorption and scattering due to the presence of cells in whole blood.^[39] **Table 2** summarizes the parameters of ECBSs for detecting biomarkers in blood and serum.

Very high glucose concentrations in the blood make it detectable using many devices available not only in laboratory environments but also on the market.^[40] Blood tests are a staple of the current medical practice for glucose detection and monitoring. For this reason, most of the studies on self-powered blood tests deal with glucose detection exploiting the strong and facile electro-catalytic conversion driven by enzymatic reactions. Self-powering is a niche topic for the research on biosensing for medical purposes and blood tests based on enzymatic biofuel cells are poorly explored in this field, although such biosensors allow conjugating devices' architectural simplicity and the ability to use biofluids based on device operation autonomously in real life. However, the richness of the blood matrix in metabolites such as glucose could be of great importance in developing sensors using biochemical reactions within the fuel cell concept.

During the last lustrum, glucose detection by self-powered biosensors has been the subject of some interesting works show-

ing an efficient outcome in the case of real blood samples. Very recent work by Sailapu et al. is targeted to self-powered glucose tests in serum responding to REASSURED criteria,^[13a] which are affordability, sensitivity, specificity, rapidity, deliverability, equipment-free, and user-friendly character, all these features in combination with a real-time operation capability.^[41] Here, it is shown a paper-based biofuel cell in the form of a smart strip, made of printed electrodes on a flexible PET substrate equipped with simplified electronics, which can measure glucose in human serum. The anode is composed of multi-walled carbon nanotubes (MWCNTs) on a silver/carbon electrode covered by a naphthoquinone-functionalized redox polyethyleneimine matrix (NQ-LPEI) containing some flavin adenine dinucleotide-dependent glucose dehydrogenase (FAD-GDH) enzyme. A glass-fiber-paper has been used as a spacer with the cathode (silver oxide/carbon paste mixture) and the sample collector. Here, a certain volume of serum sample (3.5 μL) is required on the glass-fiber-paper collector to ensure a connection between the anode and cathode. In a simple design that uses only passive circuit elements and is therefore compatible with printed manufacturing, the electronic circuit uses an open circuit voltage drop (V_{oc}) across a load resistor, which depends on the glucose diffusion through the collector. Thus, the decay rate of V_{oc} is proportional to

the concentration of glucose in the serum (the higher the glucose content, the higher the decay current due to diffusion-limited effects at the current-limiting electrode), and the electronic circuit is meant to be stored on a capacitor a fraction of the electric charge flowing into the circuit due to the current decay. The device output is then given by the voltage setting up at the capacitor plates (which is higher for growing concentrations, since the total decay charge stored by the capacitor in a given time window increases with the glucose concentration increase). In this way, a linear calibration curve consisting of the stored voltage as a function of concentration may be assessed. It is important to note that the sensitivity of ECBS can be finely tuned by properly sizing the electronic components on the printed strip.

Guan et al. have shown an interesting proof of concept consisting of an artificial blood vessel operating as a biofuel cell for the self-powered detection of glucose.^[45] In this case, a fiber-like conducting polyaniline/thermoplastic polyurethane (PANI/TPU) membrane is implemented by using the electrospinning technique. Two separate parts of the PANI/TPU membrane have been loaded with glucose oxidase (GOx) and laccase enzymes to form the anode and the cathode of the enzymatic cell. An electron transfer at the anodic interface is sustained by the GOx-mediated electrocatalytic oxidation of glucose next to the anode, leading the production of protons to be driven at the laccase-decorated cathode. Electrons reaching it from the external circuit allow laccase to catalyze the reversible oxygen reduction reaction realizing H₂O₂ production. The net effect of the process is an efficient chemical-to-electrical energy conversion. The performance of the as-prepared artificial blood vessel was tested in simulated blood, also under mechanical stress (stretching up to 200%), and showed its effectiveness in determining glucose levels in the diagnostic window of diabetes when generating a voltage of 50 mV. Thanks to the non-toxic character of PANI and TPU, the proposed device is verified to be promising as an implantable battery in blood vessels.

The work by Escalona-Villalpando et al. demonstrates a self-powered glucose sensor platform based on a flow-through PMMA microfluidic system that is aimed to improve the catalytic properties of the used biocatalysts.^[42] The proposed platform consists of a sensing unit connected to a wi-fi unit for data transmission. The sensing unit exploits an enzymatic biofuel cell consisting of a GOx/polyethyleneimine-modified toray carbon paper (TCP) bioanode and an anthracene-modified MWCNTs laccase-based biocathode. Human blood or serum may act as the anolyte and PBS at pH 5.6 is used as the catholyte. V_{oc} calculated from polarization curves acquired as a function of glucose concentration is the operational sensing parameter for the proposed device.

The first characterization round made using PBS at pH 7.4 as anolyte, has shown reproducible and promising results in the low millimolar range for glucose (linearity of the maximum current/power from polarization profiles), also in the presence of typical blood interferers dopamine (DA), uric acid (UA), and ascorbic acid (AA).^[42] The analysis using real blood as anolyte has shown the ability to measure glucose levels in blood down to about 3 mmol L⁻¹. Comparison with results obtained by a commercial glucometer (ACCU-CHEK) shows that the proposed platform underestimates glucose concentrations with a relative error not exceeding 10%–15% of concentration values obtained by the commercial testing tool.

A significant example of a real-world application of self-powered biosensors was demonstrated by Huang et al.^[47] Here, a needle-like enzymatic biofuel cell was developed and used to monitor underwater the health state of a largely farmed and consumed fish (the Tilapia). The active part of the device consists of i) a needle-like anode made of a platinum-iridium wire coated by carbon black and functionalized by a vitamin K3 layer (acting as an electron mediator) containing diaphorase (Dp) and glutamate dehydrogenase (GDH) enzymes; ii) a gas-diffusion biocathode made of carbon cloth modified by some bilirubin oxidase (BOD) and immersed in a 1% agarose hydrogel containing buffer salts (Figure 2a–c). The current/power generation is driven by the anodic conversion of glucose to NADH due to GDH followed by the oxidation of NADH to NAD⁺ (mediated by Dp), producing O₂ and 2 electrons. Electrons reach the cathode via the external circuit, favoring the O₂ reduction to H₂O catalyzed by BOD. To complete the proposed platform, the cell is connected to a charge pump circuit whose output biases an LED indicator. The anode is inserted into the caudal area of the fish and the cathode is protected in a hermetically sealed bag and left outside the fish's body. Within this scheme, the power generated from the system due to the two steps reaction at the anode followed by an oxygen reduction at the cathode (being accordingly the overall reaction, proportional to the glucose level near the anode), controls the process of charging and discharging the capacitor in the charge pump regulator. In turn, the charge/discharge process is visualized by the LED as a blinking frequency, which is proportional to the glucose levels activating the power generation. Then, a smartphone is used to record the blinking frequency through a freely available mobile app, i.e., the MudWatt Explorer. A maximum V_{oc} of 0.43 V (power density generated: 11 μW cm⁻²) is produced by the cell at a glucose concentration of about 1 mmol L⁻¹ (or 180 mg dL⁻¹), while a dynamic linear response to glucose is found in the concentration window from 500 μmol L⁻¹ to 10 mmol L⁻¹.

Another popular high-concentration metabolite, such as lactate was also detected using commercially available blood tests. However, during the last lustrum, lactate was not detected using self-powered biosensors. On the one hand, lactate excess does not impact health as glucose does, so its monitoring is not a pre-rogative for medical diagnostics in terms of the global burden of disorders due to hyperlactatemia.

Cholesterol in platelet-poor plasma prepared from whole blood has been detected by a self-powered biosensor consisting of a fuel cell made of carbon cloth electrodes acting as anode and cathode (Figure 2d,e).^[48] The anode is modified with a sol-gel membrane of phenothiazine (PTZ) containing the cholesterol oxidase (ChOx) enzyme, while the carbon cloth cathode is coated by a Prussian blue (PB) membrane containing ChOx. Two reactions are involved in this biofuel cell. An electrocatalytic reaction occurs at the anode due to the oxidation of cholesterol mediated by the PTZ matrix. Hydrogen peroxide is formed at the cathode due to the reduction of oxygen to H₂O₂ as a result of the oxidation of cholesterol to cholestenone, catalyzed by ChOx. H₂O₂, the concentration of which is proportional to the cholesterol concentration, is then monitored at the PB-coated cathode (sensing electrode). Using this cell architecture, a cholesterol quantification both in PBS buffer solution and in plasma of healthy volunteers was assessed both from variations of the V_{oc} and faster variations of the short circuit current, which were

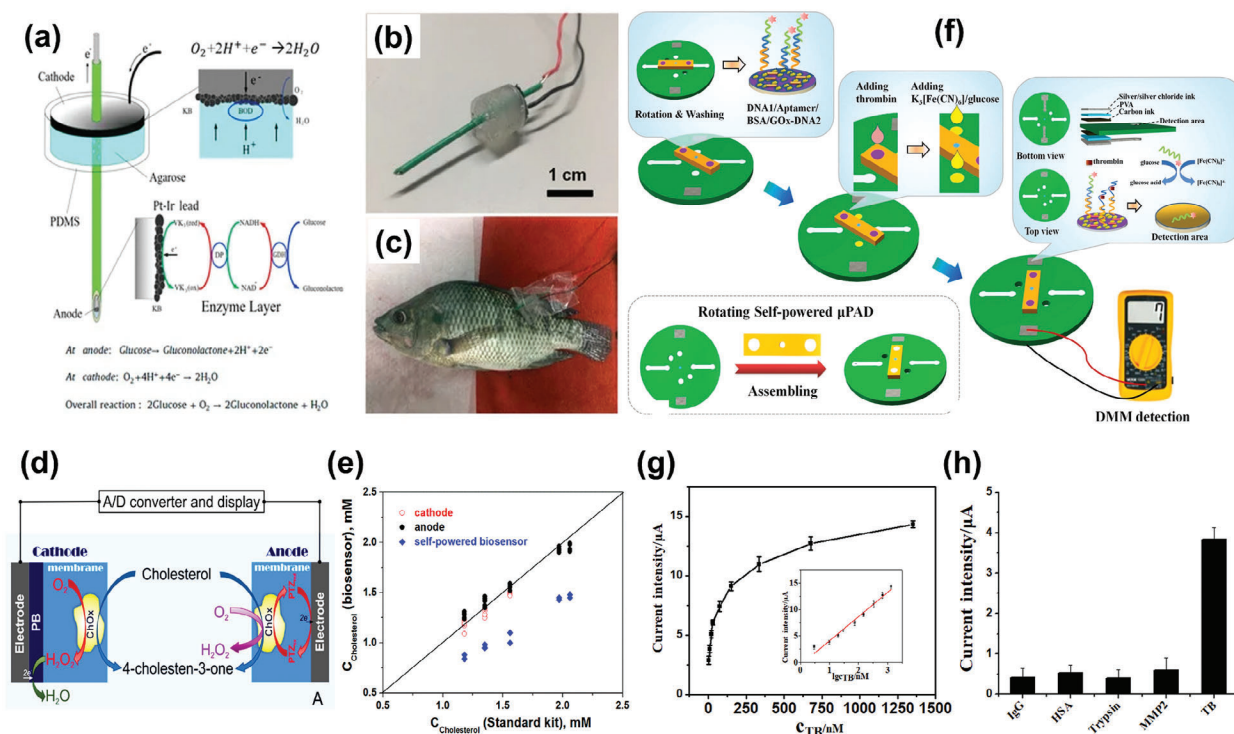


Figure 2. a) Schematic structure of the needle-type enzymatic biofuel cell and schemes of glucose oxidation at the anode along with O_2 reduction at the enzymatic gas-diffusion cathode. b, c) Images of the needle-type enzymatic biofuel cell and the needle-type enzymatic biofuel cell inserted into a living fish (*Tilapia*) around the caudal area to access biofuels and a gas-diffusion biocathode sealed in an airtight bag filled with air, respectively.^[47] d) Scheme of the single-enzyme-based self-powered membrane-free cholesterol biosensor. e) Comparative free cholesterol quantification in plasma. (○) Cathodic system on SPE; (●) anodic system on SPE; (◆) self-powered biosensor on CCEs. Reproduced with permission,^[48] Copyright 2014, American Chemical Society. f) The rotational paper-based device and use for DMM detection. The integration of valves through “ON/OFF” states can help realize the function of rinsing, incubation, and reaction for the self-powered EBFC sensor. g) The self-powered paper-based microfluidic chips detect the response curve of the ammeter with different concentrations of thrombin (3, 10, 20, 30, 75, 150, 335, 675, 1350 nM). The inserted illustration is the quantitative curve of the DMM signals. h) Selectivity of thrombin was investigated on μPADs , and matrix metalloproteinase 2 (MMP2), trypsin, Immunoglobulin G (IgG), and Human Serum Albumin (HAS) were selected as the interference agents, and these interference agents are all 1000 nM, respectively. The concentration of thrombin solution was selected as 10 nM. Reproduced with permission,^[49] Copyright 2021, Elsevier.

influenced by the cholesterol dose-dependent cathode reaction upon the addition of cholesterol aliquots in the analyzed matrices. In the latter case (short circuit analysis), authors demonstrated an increased dynamic range (linear response of short circuit current vs cholesterol concentration) in a concentration range from 0.15 mmol L^{-1} to 4.1 mmol L^{-1} (a range that is compatible with the analysis of undiluted serum samples) a better sensitivity ($26.0 \pm 0.5 \text{ mA mol L}^{-1} \text{ cm}^{-2}$) and a limit of detection (LOD) of $1.4 \mu\text{mol L}$, calculated following the IUPAC standard from the linear regression of the calibration curve as $3\sigma_{\text{slope}}/\text{sensitivity}$. Herein, σ_{slope} is the standard deviation of the slope (or the system sensitivity) of the linear best fit to the calibration curve. A linear correlation was also found with the response of the standard kit (BioVision Cholesterol/Cholesteryl Ester Quantitation Kit II).

Trypsin exhibits activity in an alkaline environment, especially in the presence of calcium (Ca^{2+}), magnesium (Mg^{2+}), and manganese (Mn^{2+}) ions.^[51] This feature was used to develop a self-powered biosensor for real-time detection of trypsin in body fluids. The fabricated device consists of two half-cells connected by an agarose bridge containing potassium chloride (KCl) as the electrolyte.^[50] One half-cell acts as a cathode (site of reduction)

for iron ions (Fe^{3+}), and the other acts as an anode (site of oxidation) for magnesium ions (Mg^{2+}). Before introducing the analyte (trypsin), a passivation layer of aluminum prevents the two cells from discharging. The passivation layer is etched by adding the analyte and sodium hydroxide (NaOH), which exposes the magnesium anode to the electrolyte bridge, effectively completing the electrical circuit and generating current. This approach offers a simple and specific method for detecting trypsin. Notably, the current generated can even power a light-emitting diode (LED). Moreover, it correlates with trypsin concentration, with a LOD of $0.5 \mu\text{g mL}^{-1}$. However, the sensor has limitations. It is intended for single use only and has a long reaction time (up to 3 h) due to the need to incubate the analyte in a gelatin solution.

Another model molecule for biosensing is the thrombin, a pro-coagulant enzyme also involved in the homeostasis of blood vessels. Although blood normal levels are in the nanomolar range (from 1 to 500 nmol L^{-1}),^[52] its role in biosensing has been fostered by the explosion of the aptamers, which are short oligonucleotides from synthetic DNA, RNA, XRA, or peptides able to bind the related target molecules with an enhanced specificity. Aptamers are currently used as outperforming biorecognition elements in biosensors and, historically, the first anti-thrombin

aptamer, known as TBA, was developed shortly after introducing this new concept for tailoring a high-affinity recognition in biosensors. Recently, Li et al. reported a self-powered paper-based microfluidic chip to detect thrombin.^[49] The device consists of two parts interfaced with each other and free to rotate around a central axis perpendicular to their surfaces (Figure 2f). The upper part is a reaction disk hosting two circular-shaped hydrophilic reaction areas decorated by Au nanoparticles (NPs) coated by a sandwich-like structure made of i) a thiolated DNA sequence bond to Au NPs using an Au-sulfur interaction; ii) a second DNA sequence modified by GOx (GOx-DNA); iii) the thrombin aptamer HD22 linking the DNA sequences to form the sandwich. The lower part is a paper-based disk equipped with two supercapacitors whose plates, made of Ag/AgCl/polyvinyl alcohol/carbon structures, are deposited by printing routes on both sides of the paper disk layer. Upon rotating the reaction area, the reaction disk may be positioned in correspondence with the bottom plate of the capacitor. In this framework, the analyte detection can be implemented as follows. Upon exposure of the reaction area with diluted serum samples from the whole blood of healthy volunteers spiked with thrombin aliquots. The thrombin-HD22 interaction releases the GOx-DNA, which is transported toward the detection area previously dipped with a potassium ferricyanide-glucose solution in PBS. GOx interaction with glucose allows its oxidation and consequent reduction of iron ions in ferricyanide solution ($\text{Fe}^{3+} \rightarrow \text{Fe}^{2+}$) leading to the formation of ferrocyanide and to a concentration change of ferricyanide that is proportional to the thrombin content in serum. Electrons generated from glucose oxidation are collected and measured in an amperometric scheme for analyte quantification and, at the same time, they allow the supercapacitor charging. The fabricated device allowed to collection of a lin-log calibration curve in a thrombin concentration range between 3 nmol L^{-1} and $1,35 \mu\text{mol L}^{-1}$ (Figure 2g–h), with the LOD of 0.9 nmol L^{-1} estimated by the signal-to-noise ratio criterion ($S/N > 3$).

Even if power generation is affected by several factors, using metabolite-rich biometric data in blood makes ECBSs very promising for fabricating self-powered blood monitoring systems. However, most studies were performed on developing self-powered ECBSs for glucose detection (Table 2). Several biomarkers present in blood (Table 1) have not yet been used to evaluate self-powered biosensing systems. Unfortunately, detailed information on the stability of these devices is not available, which could be the subject of future investigations. Preparing new electrode structures and their functionalization with appropriate additive materials could provide effective solutions for producing electrochemical systems and their application in detecting other biomarkers in the blood. Thus, future research efforts are needed to explore new electrode materials and develop effective functional strategies for a more accurate evaluation of the feasibility of self-powered ECBSs in blood monitoring.

2.2. Monitoring of Sweat

Acids, peptides, proteins, metabolites, and hormones enter the sweat from the blood and interstitial fluid. Sweat is therefore composed of biomarkers and has been considered a suitable electrolyte for developing electrochemical sensors and their applica-

tion in non-invasive diagnostics of several diseases.^[13b] From a biological perspective, sweat is a biofluid produced by sweat glands and carried to the epidermis surface via secretory ducts. Sweat glands are found in the dermis layer of the skin all over the body and, based on location, structure, and function, are divided into eccrine, apocrine, and apocrine glands. Each type of sweat gland secretes different amounts and quality of biomarkers. Therefore, the detection of specific metabolites and drugs depends largely on the sampling site in the body. Apocrine and apocrine sweat glands are limited to areas of the body such as the axilla, while eccrine glands are the most numerous sweat glands, distributed over almost the entire surface of the body and open freely to the surface of the epidermis. The sweat produced by eccrine glands is readily available and can be collected from children and adults at convenient sites on the body in a non-invasive and on-demand manner (e.g., through local chemical stimulation). This type of sweat contains water and various electrolytes and can be released directly onto the surface of the skin.^[53] The amount of sweat produced can change based on the individual's physical condition and can be monitored by electrochemical sensing methods. Sweat monitoring systems can be positioned close to the source of sweat production to quickly detect analytes before they are degraded. Quantitative in-situ sweat analysis is important for monitoring physiological health status and diagnosis of diseases.^[54]

2.2.1. Biomarkers in Sweat

Sweat is produced by sweat glands to regulate body temperature and to moisturize and protect the skin. It is 99% water and contains a wide range of critical biomarkers that can indirectly or directly reflect human health and thereby help track disease progression. Table 3 reports the main biologically significant markers and their concentrations in human sweat. Chemicals present in sweat (Figure 3) can be classified into three types: electrolytes (Na^+ , K^+ , Cl^- , NH_4^+ , Zn^{2+} , and Cu^{2+}), metabolites (glucose, cortisol, lactate, urea, and ethanol), and macromolecules (cytokines, peptides, and proteins).^[54] Na^+ and Cl^- ions are the predominant electrolytes found in human sweat and play a key role in determining the amount of water present in sweat, which is essential for calculating sweat rate. Simultaneously, the concentration of Na^+ in sweat influences the body's electrolyte levels and plays a crucial role in maintaining osmolality, hydration, and pH levels.^[55] The range of Na^+ concentrations under normal physiological conditions is 10–100 mM, but large losses of Na^+ in a patient's sweat may indicate hyponatremia, electrolyte imbalance, or dehydration. These conditions can harm human health and reduce physical and mental performance.^[56] Sweat chloride analysis is considered the most reliable method for identifying cystic fibrosis, a genetic disease characterized by the production of thick and sticky mucus due to increased concentrations of chloride in the extracellular fluid that affects the lungs, pancreas, and other organs.^[57] Sweat-based biomedical technologies are considered effective non-invasive approaches for analyzing fibrosis progression.

Schematic representation of the anatomical structure of human sweat glands (eccrine, apocrine, and apocrine) and the sebaceous gland within a cross-section of the skin. Sweat, released from sweat glands, is transferred to the epidermal surface via

Table 3. Main biologically significant markers and their concentrations in human sweat.

Biomarker	Concentration	Disease	Refs.
Na ⁺	10–100 mM	hyponatremia, electrolyte imbalance, dehydration	[56a]
Cl ⁻	10–100 mM	Dehydration, cystic fibrosis	[58a]
K ⁺	1–18.5 mM	Dehydration, muscle cramps	[56b,59]
Ca ²⁺	0.3–10 mg dL ⁻¹	Acid-base balance disorder, myeloma, cirrhosis, normocalciuric hyperparathyroidism, renal failure	[61–63]
NH ₄ ⁺	0.5 e 25 mM	Muscle fatigue	[77]
Cu	≈0.5–1.5 mM	Menkes' and Wilson's disease	[64]
Glucose	0.06–0.2 mM	Diabetes, hypoglycemic shock	[59,78]
Lactate	10–25 mM	Heart failure, liver failure, renal failure, cystic fibrosis	[67,69]
(AA	10–50 mM	Tumors, cancer, kidney disease, thrombosis stones	[75]
Ethanol	0–100 mM	Inebriation	[73a,79]
Cortisol	8,16–141,7 ng mL ⁻¹	Hypoglycemia, elevated blood pressure, hyponatremia, electrolyte disturbance, obesity, fatigue, post-traumatic stress disorder	[70]
IL-6	10.0 ± 2.2 pg mL ⁻¹	Depression	[76]

secretory ducts. The magnification of an individual drop of sweat illustrates the list of major sweat biomarkers, divided into electrolytes, metabolites, and macromolecules.

For both newborns and adults, a sweat Cl⁻ level of ≥ 60 mM confirms the presence of cystic fibrosis, while a sweat Cl⁻ below 30 mM suggests that cystic fibrosis is improbable.^[58] Potassium is crucial for the functionality of nerve and muscle cells, as well as for carbohydrate metabolism and cellular biochemical reactions. Sweat contains 1–18,5 mM K⁺. Excess potassium loss through sweat can indicate dehydration, which not only causes muscle

cramps but can also be life-threatening in patients with cardiovascular disease.^[56b,59] The calcium concentration in sweat can vary greatly, with levels typically ranging from 0.3 to 10 mg dL⁻¹ and averaging around 5 mg/dL. Increased variability is probably caused by the location of the sample, surface contamination, and varying levels of perspiration.^[60] Monitoring sweat Ca²⁺ levels is important to control the risk of hypocalcemia and predict diseases like acid-base imbalance, cirrhosis, myeloma,^[61] renal failure,^[61–62] and normocalciuric hyperparathyroidism.^[63] Copper (Cu) is a crucial redox metal for the majority of living organisms. Indeed, redox catalysis, oxygen transport, and electron transfer are just a few of the basic biochemical activities that nature has adapted to rely on the redox cycle between Cu⁺ and Cu²⁺. On the other hand, this redox capability can also be risky as the Cu redox cycle efficiently triggers the production of reactive oxygen species (ROS), leading to oxidative damage to biomolecules. Specific measurement of the metabolic Cu pool in sweat is of increasing interest for the study of copper metabolism and also as a potential diagnostic tool. The concentration of Cu in sweat is ~0.5–1.5. Changes in Cu concentrations can cause Menkes' disease (MD) and Wilson's disease (WD).^[64]

Glucose is among the main metabolites in human sweat. The level of glucose in human sweat ranges from 0.06 to 0.2 mM. Furthermore, sweat is the most accessible form of glucose because it offers a wide range of sampling locations outside the body, easy placement of devices, and contains electrolytes and metabolites relevant to the body's functions. Because sweat offers the greatest number of sample sites outside the body, continual access, simplicity of device implantation, and the presence of physiologically relevant electrolytes and metabolites, it is the most readily available source of glucose.^[65] Therefore, sweat glucose testing may be an alternative to blood glucose analysis. Unlike blood glucose measurement, sweat monitoring is a non-invasive approach. Sweating happens rapidly and sweat glands have a good blood supply, allowing for the evaluation of glucose levels using sweat samples.^[65b] Thus, self-powered sweat-based glucose sensors can be an effective solution for indirectly determining blood glucose levels. Nevertheless, there are notable obstacles in acquiring precise sweat glucose data because of fluctuations in environmental

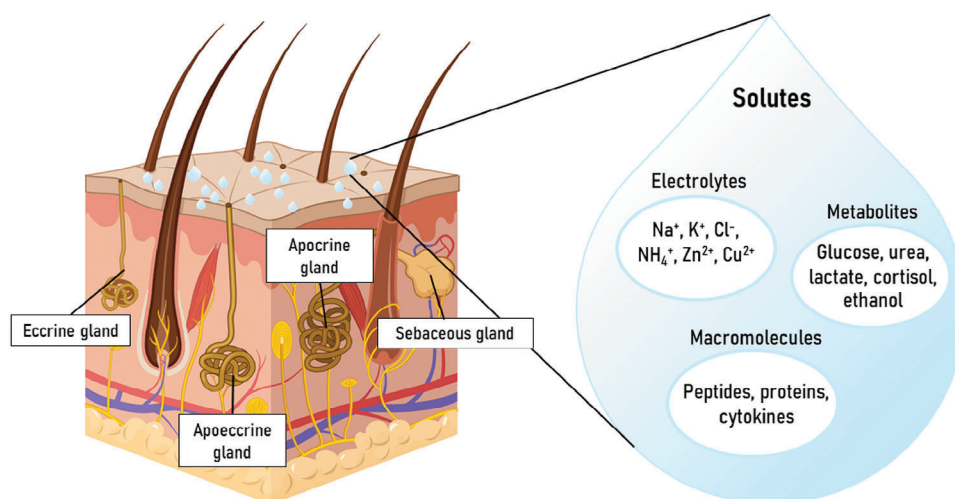


Figure 3. Schematic representation of sweat components. Created with BioRender.com.

factors like temperature, skin impurities, irregular sampling without iontophoretic stimulation, limited capacity, and combining previous samples with fresh ones. Furthermore, monitoring sweat glucose levels is very challenging because of its low concentration, making highly sensitive devices necessary.^[66]

Acetate is the most important metabolite of anaerobic respiration. It is produced during anaerobic activities such as high-intensity exercises. Determination of lactate in sweat plays an important role in treating some critically ill patients, as it provides information for detecting diseases such as renal, heart, and liver failure. Moreover, studies have been conducted using sweat lactate as a marker for cystic fibrosis (as it also results in a reduction of available oxygen).^[67] Regarding physical activities, lactate levels can be estimated to determine the human health status after exercise.^[68] The lactate concentration range for a healthy person is 10–25 mM, which can differ based on gender and age. Its high levels, leading to increased sweating, can be a sign of tissue damage.^[69]

Sweat includes not only ions and molecules but also hormone-like molecules and low molecular-weight proteins like cortisol, cytokines, and neuropeptides. Non-invasive detection of cortisol in sweat has received much attention in recent years. Biochemical analysis of this component has become an important basis for quantifying stress and stress-related diseases. Cortisol is a glucocorticoid secreted by the adrenal cortex, which is essential for maintaining the balance and stability of physiological functions in patients under severe psychological stress. In reaction to environmental stress or fear, the adrenal glands release it as the end product of the hypothalamic-pituitary-adrenal (HPA) axis activation cascade. Human sweat cortisol concentrations range from 8.16 to 141.7 ng mL⁻¹, and abnormal cortisol levels in patients typically result in hypoglycemia, increased blood pressure, hyponatremia, electrolyte disturbances, obesity, fatigue, and post-traumatic stress disorder.^[70]

Other biomarkers, such as ethanol, drugs (e.g., nicotine or levodopa), and vitamin C, are also used for therapeutic, nutritional, and abuse purposes. The metabolism of ethanol has been studied extensively in humans because it is the key molecule that causes intoxication when drinking alcohol in excess. Blood and urine are the most prevalent biological samples for analyzing alcohol consumption. Although this method provides very accurate measurements of blood alcohol concentration (BAC), it requires invasive data collection methods and cannot be performed on-site.^[71] Breath alcohol concentration measurement was subsequently developed because it showed a good correlation with blood alcohol levels. The advantage of sweat testing as an alternative to blood and breath tests is that it contains compounds that can function as biomarkers without requiring traditional invasive testing techniques.^[71–72] Experimental findings indicate a correlation between the levels of ethanol in blood and sweat, which could enable the continuous monitoring of blood-alcohol levels through sweat analysis.^[73] The concentration of ethanol detected in sweat may depend on the amount of alcohol consumed.

Measuring vitamin C (or AA) in sweat can provide valuable information about an individual's antioxidant status. Currently, AA is measured using expensive blood tests requiring trained personnel. Instead, sweat sampling is a cost-effective and non-intrusive method for detecting AA. The relative concentration of AA in sweat varies from 10 to 50 μmol L⁻¹, and its abnormal con-

centration indicates certain human diseases.^[74] For example, tumors, cancer, kidney diseases, and thrombosis.^[75]

IL-6 was found in eccrine sweat. The concentration of IL-6 in sweat is 10.0 ± 2.2 pg mL⁻¹. In addition, monitoring IL-6 levels in sweat can help manage the risk of depression. Individuals diagnosed with depression had a mean of 133.8 pg mL⁻¹ IL-6 found in their sweat, a level that was notably elevated compared to individuals without the disorder.^[76]

2.2.2. Detection of Biomarkers in Sweats

Research studies indicate a correlation between the levels of sweat and blood glucose, which can be a critical factor in managing diabetes.^[78,80] Furthermore, in enzyme-based ECBSs, bioenergy is converted into electrical energy, which enables the development of self-powered detection systems. Here, glucose can be used as a fuel and sweat serves as an electrolyte for self-powered biofuel cells. **Table 4** reports the parameters of ECBSs for detecting biomarkers present in sweat. Recent studies indicate that fabricating composite electrode structures based on functional nanomaterials is an efficient strategy to enhance their performance. Enzyme loading can be improved by using specific nanostructures with a large surface area as a support. In addition, the application of nanomaterials can improve the stability and functionality of enzymes in biofuel cells. For example, DNA-templated silver (Ag) nanoclusters with their excellent electronic properties, facilitate efficient charge transfer between the GOx enzyme and the electrode during redox reactions.^[7] Ag nanostructures readily donate and accept electrons during redox reactions, and these processes are reversible. Cyclic voltammetry (CV) tests were carried out. The anodic peak values were used to calculate the current density, which was increased with glucose concentration. The LOD of the sensor was 29 μM. This value is significantly lower than the glucose concentration in the body's biofluids. Here, the current density increases with the concentration of glucose showing a nonlinear dependence. The obtained results suggest that the enzymatic reactions control the electrochemical processes. Enzymes catalyze the oxidation of glucose enhancing the kinetics of biomarker capture. Thus, the functionalization of the working electrodes with glucose enzymes speeds up the sensing reactions and enables selective detection of glucose in sweat. Furthermore, the nanomaterials were prepared on electrode substrates by screen printing technique, which is another advantage for developing modern self-powered sensing technologies.^[7]

Advances in research into portable electronic devices are opening up new solutions for self-powered detection systems. The coupling of flexible photovoltaic cells with environmentally friendly and lightweight zinc manganese oxide (Zn-MnO₂) batteries was used to power an enzyme-based ECBS for real-time sweat glucose detection. However, in the first stage of glucose tests, the amount of sweat collected was insufficient and the output signal was not stable. The required amount of sweat for accurate determination of glucose was achieved after 10 min of physical activity.^[13b] However, the concentration of ions (e.g., Na⁺ and K⁺) also increases due to physiological activities. Therefore, the reaction current can be influenced by inorganic ions. To overcome this issue Lu et al. proposed using compensation electrodes by isolating them with membranes.^[81] In addition, their findings

Table 4. Parameters of ECBSs for the detection of biomarkers in sweat.

Anode material /Working electrode	Cathode Material /reference	Biomarker/Biofluid	Concentration/detection range	LOD	Output	Detection method	Refs.
NA	^{a)} DNA-templated AgNCs/GOx	Glucose	<200 μM	29 μM	NA	Electrochemical reaction	[7]
^{b)} Au/Prussian blue/GOx	Au/AgAgCl	Glucose	50–200 μM	NA	Current 3.18 nAmM^{-1}	Electrochemical reaction of glucose	[13b]
^{b)} Au/Chitosan/NiCo ₂ O ₄ nanowires	AgAgCl	Glucose	5–25 mM	10 μM	Current 0.5 mAmM^{-1}	Oxidative reaction of glucose with Ni and Co nanowires	[81]
NA	NA	Glucose/ artificial sweat	10 nM to 50 μM	1 nM	NA	Chronoamperometry	[65b]
LDH/RGO-CNT/TMC	^{a)} RGO-CNT/TMC	Lactate/artificial sweat	0–10 mM	9.49 μM	Current 18.46 mAmM^{-2}	Impedance spectroscopy	[68]
^{b)} Graphene-modified polyimide film	NA	Ascorbic acid (AA)	NA	66 μM	<current 0.015 mAmM^{-2}	Square wave voltammetry (SWV) and Chronoamperometry (CA)	[75]
Mg functionalized aptamers with V ₂ CT _x MXene, Co, and Ni	^{a)} Ag/AgCl ^{a)} Zinc	Artificial sweat Cortisol	NA From 10 fg mL^{-1} to 100 ng mL^{-1}	NA 0.17 fg mL^{-1}	NA NA	Electrochemical reaction Electrochemical sensing	[9] [70c]

^{a)} (Working electrode); ^{b)} (Reference electrode).

indicate that enzyme-free electrodes can be integrated with supercapacitors for self-powered monitoring of glucose (Figure 4a). This is a promising achievement to extend the lifetime of the sensing device.

Metal cobaltites with their attractive electrical and electrochemical properties were used for fabricating electrodes and their integration into ECBSs. The electrical conductivity and electrochemical activity of nickel cobaltite (NiCo₂O₄) nanomaterials are significantly higher than pure cobalt and nickel oxides (Co₃O₄ and NiO).^[82] The experimental results show that electrodes based on NiCo₂O₄ nanowires can be successfully used in the architecture of miniaturized micro-supercapacitors and electrochemical sensors for sweat monitoring. The material retained 96% of its initial capacitance value after 20 000 cycles (Figure 4b). The presence of Ni and Co in the electrode material of the ECBS significantly affects the oxidation of glucose and the response current of the sensing system was varied as a function of glucose concentration (Figure 4c). The detection limit of the sensor was 10 μM . These results show that NiCo₂O₄ nanowires are promising structures for the fabrication of self-powered ECBS and the detection and quantification of glucose in sweat. Wherein, enzyme-free electrodes can facilitate the fabrication of ECBSs and extend their lifetime.^[81]

Thermoelectric generators (TEGs), in which the temperature difference between the environment and the human body is converted into electrical energy, were also used in self-powered ECBSs for glucose detection. However, the temperature difference should be sufficient to generate the energy required by ECBS.^[65b] Here, the electrochemical system is activated by thermoelectric fabrics. The ECBS and TEG were fabricated using cotton and poly(3,4-ethylenedioxythiophene):poly(styrenesulfonate)/dimethylsulfoxide/(3-glycidioxypropyl) trimethoxysilane (PDG) yarn.

This structure is both lightweight and stable for bending. The detection signal was achieved by maintaining a temperature variance of 2.2 K between the human body and the surroundings. In this case, the working electrode was also functionalized with the GOx enzyme for selective glucose detection, and the sensor showed a linear dependence on glucose concentration.

A composite material of reduced graphene oxide (RGO) and carboxylated MWCNTs was fabricated on cellulose fibers.^[68] To produce the anode and cathode, the electrodes were functionalized with lactate dehydrogenase and laccase, respectively. The performance of the system was studied by impedance spectroscopy (EIS). The RGO and MWCNT, which have high conductivity, reduced the resistance of the electrodes and enhanced the charge transport. However, the enzyme coating for selective detection of lactate partially increased the transfer resistance of the electrons. In addition, the electrochemical response of the system was measured at different lactate concentrations (0–100 mM). The redox reactions improved with the lactate concentration, which was saturated above 80 nM. The current density of the sensor retained 95% of the initial value after 300 bends and 83% after 30 days of operation. The effect of lactate concentration on the power output of the BECS was also investigated. The system achieved a maximum power of 18.46 $\mu\text{W cm}^{-2}$ at a lactate concentration of 10 mM. Thus, each component in the electrode design plays a critical role in the sensing characteristics and power output of the self-powered ECBS. Graphene prepared on polyimide substrates was used for the electrochemical detection of AA in artificial sweat, where the LOD of the sensors was 66 μM .^[75] In this case, the selectivity of the working electrode needed further investigation and the system was operated with solar cells. In another work, solar cells and rechargeable batteries were combined

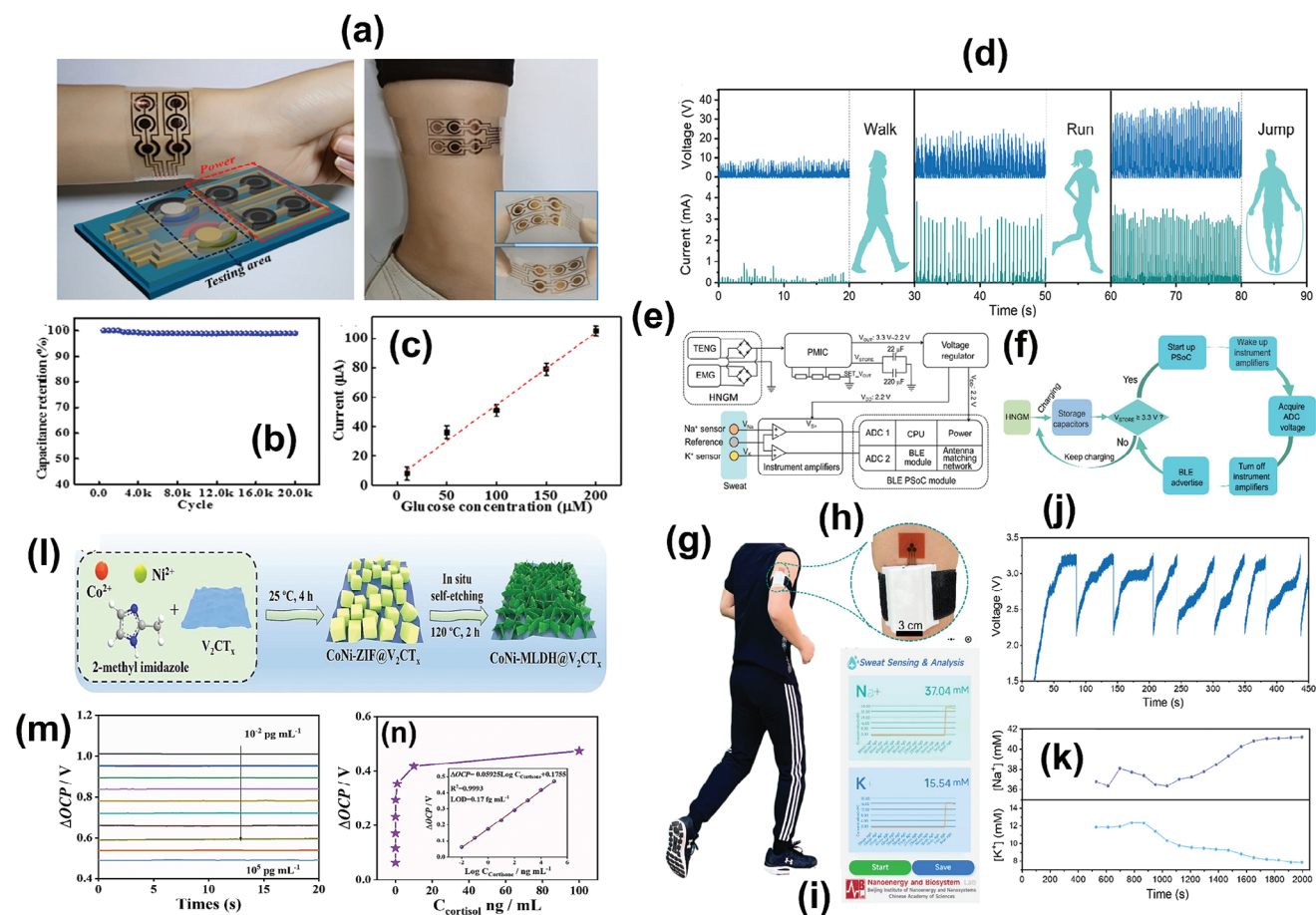


Figure 4. a) Schematic illustration of transection for glucose sensor, compensation electrode, $[Na^+]$ and $[K^+]$ sensors. Mode 1 is amperometric sensor and the Mode 2 is the capacitance-type sensor. b) Variation of capacitance stability of MSCs with 20000 cycles. c) Linear relationship of responsive current versus glucose concentration. Reproduced with permission,^[81] Copyright 2019, Elsevier. d–k) Real-time on-body sweat sensing and data transmission powered by hybrid nanogenerator modules. (d) Output performance of energy harvesting devices during walking, running, and jumping. (e) Module diagram of the self-powered wearable sweat analysis system (SWSAS). (f) Operation flow of the SWSAS. (g) A photograph of an individual with the SWSAS strapped to the arm during running. The SWSAS wirelessly senses Na^+ and K^+ in sweat via Bluetooth and records the data to a mobile phone. (h) A photograph of SWSAS strapped to the arm. i) Mobile phone interface of sweat sensing and analysis developed based on the WeChat applet. (j) Real-time potential of the capacitor charged by an HNGM. (k) The real-time concentration of Na^+ and K^+ in sweat during running by using SWSAS. Reproduced with permission,^[87] Copyright 2022, John Wiley & Sons. (l) Schematic illustration of the preparation process of the Schottky $CoNi-MLDh@V_2CT_x$ heterojunction. (m) $OCP-I$ curves of the constructed self-powered aptasensor for the detection of cortisol with different concentrations (10 fg mL^{-1} , 0.1 pg mL^{-1} , 1 pg mL^{-1} , 10 pg mL^{-1} , 100 pg mL^{-1} , 1 ng mL^{-1} , 10 ng mL^{-1} , 100 ng mL^{-1}). (n) Relationship between the caused ΔOCP and the cortisol concentration. Reproduced with permission,^[70c] Copyright 2023, Elsevier.

with ECBS to estimate the pH value of sweat.^[83] The aforementioned sensing systems were considered self-powered. However, it is worth noting that in these approaches, power is not generated in the ECBS device by electrochemical energy conversion or by converting mechanical energy into electrical energy, as in triboelectric nanogenerators.

Artificial sweat is also used to evaluate the performance of self-powered sensor devices.^[9,84] A battery system in which artificial sweat (an aqueous solution of NaCl and lactic acid) performs the function of a biofluid was studied. Magnesium (Mg) and Ag/AgCl were used as anode and cathode, respectively.^[9] In this case, the separator was a dry cellulose membrane. In the absence of biofluid, the electrochemical cell is in an open circuit state, and when the membrane absorbs sweat, the circuit is closed. The operating voltage provided by this design was $\approx 1.6\text{ V}$.

However, ambient temperature and sweat amount can affect the cell capacitance.

Another promising approach is the development of hydroelectric generators in self-powered ECBS where the electrical energy is generated through the interaction of a liquid with a solid surface. In this case, electrostatic interactions lead to the migration of counter ions to the surface, creating a gradient in their concentration. This streaming potential is used to generate electricity in hydroelectric generators.^[85] For example, silicon nanowires were functionalized with carbon NPs to increase the charge density at the electrode surface and improve the generated electrical energy.^[86] The performance of the electrode was investigated in an aqueous NaCl solution using the open-circuit potential method. The V_{oc} and the short-circuit current (I_{sc}) decreased with increasing NaCl concentration and showed a linear dependence.

In this case, the sensitivity of a hydroelectric device depends on the Debye length and the channel width. The Debye length is determined by the quantity of ions present in the solution. The desired current values can be achieved by connecting hydroelectric devices in parallel or in series. Experimental analyses with volunteers showed that the V_{oc} decreases with increasing exercise duration, which was attributed to the body dehydration and electrolyte concentration. The authors also suggested that the selectivity of the sensor in such a system can be tuned by modifying the surface of nanowires with ion-selective membranes for the specific binding of certain ions.

A triboelectric nanogenerator, in which the energy of body movement is converted into electricity, was also successfully used to develop self-powered ECBSs.^[87] Here, the power device is a combination of triboelectrification and electrostatic induction. The sensor patch was developed on polymeric substrates. Solutions of NaCl and KCl were used as electrolytes. The sensor response was studied to Na^+ and K^+ ions. The use of artificial sweat allows for testing the sensitivity of the sensor at the desired analyte concentration at the laboratory level. Moreover, this study also suggests that integrating selective membranes into cellular architecture enhances their selectivity. Tests on volunteers (Figure 4d–k) showed that a sufficient concentration of sweat was collected and accurate determination of the analyte was possible after 9 min of running, which confirms previously reported findings.^[13b] Hence, accurate health monitoring by analyzing biomarkers present in sweat requires time on the order of several minutes.

Advances in printing techniques make it possible to prepare electrode materials and control their shape and thickness at relatively low operating temperatures. These technologies open up new possibilities for manufacturing electrodes based on paper materials. For example, $ZnCl_2$ and polyvinyl alcohol (PVA) were deposited on filter paper using an inkjet printing process, whereby the porosity of the paper improves the adhesion of the material to its surface.^[88] Electrochemical characterization of the electrodes showed that the current generation varied depending on the humidity conditions in the cell, which is a good performance for functioning as a self-powered system. The bending partially affected the shape of the prepared electrode materials. However, the ECBS showed a quite stable sensor performance when the bending angle was increased to 180° .

More recently, the effect of immobilizing functional aptamers on composite electrodes based on V_2CT_x , MXene, Co, and Ni for selective cortisol detection was investigated (Figure 4m,n).^[70c] EIS measurements showed that the electrochemical sensing response increased with increasing cortisol concentration, which is important for analyte quantitation. However, the ECBS response was saturated when cortisol concentrations exceeded 10 ng mL^{-1} . In addition, immobilization of the aptamer affected charge transfer and reduced the output voltage due to the formation of a cortisol complex with the aptamer. These results seem to suggest that the effect of aptamer concentration on ECBS functionality and energy production should be carefully studied to find the optimal electrode composition.

Overall, various organic and inorganic nanomaterials have been studied to detect biomarkers in sweat. The application of nanostructured semiconductor materials in the architecture of electrodes may enhance the electrochemical response and selec-

tivity of sensors. Furthermore, appropriate modification of the morphology and the structure of semiconductor nanomaterials may improve the charge transport and increase the charge density at the electrode surface. The use of enzymes, aptamers, and selective membranes has a significant effect on the sensitivity and selectivity of sensors. However, the influence of each component in the electrode structure needs to be investigated in detail to optimize the performance of ECBS systems and power generation. Various approaches, such as electrochemical energy conversion, hydroelectric and TEGs, and flexible photovoltaic cells can be considered to operate ECBS for sweat monitoring. As with blood monitoring, research into the development of ECBS for sweat analysis has primarily chosen glucose as the target analyte. Some studies have also examined lactate, cortisol, and AA (Table 4). Therefore, further experimental and theoretical studies are needed to explore new electrode materials for the selective detection of other biomarkers present in sweat. Another important issue is the stability of ECBSs for sweat monitoring, which needs to be investigated in detail.

2.3. Monitoring of Saliva

Saliva is a sophisticated liquid made by the parotid, submandibular, and sublingual glands, in addition to 600–1000 smaller salivary glands. It consists mainly of water (>99%) and several minor components with important metabolic functions, such as electrolytes, immunoglobulins, proteins, enzymes, and mucins. Gingival crevicular fluid, microorganisms, desquamated epithelial cells, and food debris are also present in saliva.^[89] Thus, this biological fluid performs several important functions in the human body. Thanks to water, it moisturizes and cleanses surfaces of the oral cavity, making the texture of saliva sticky. Electrolytes are important to neutralize acid and protect teeth. Finally, organic matter promotes antimicrobial activity, tissue repair, digestion, and salivary sac formation. Therefore, saliva is important for non-invasive diagnosis and monitoring of diseases. Moreover, recent years have seen an increase in research into changes caused by environmental exposures, such as air pollution and smoking, as well as the diagnosis and evolution of diseases.^[90] Several biomarkers can be detected in this matrix, and since sampling is fast, simple, and performed using noninvasive methods, it is also used for large-scale epidemiological studies. Collected samples can be divided into stimulated whole saliva, extracted using paraffin chewing gum, and unstimulated whole saliva, collected by passive salivation or oral swab to sample a specific area.^[91] According to the sampling procedure, the presence of biomarkers in the samples varies greatly due to changes in salivary flow rate and protein secretion.

2.3.1. Biomarkers in Saliva

There are several types of DNA biomarkers such as DNA methylation, cell-free DNA, circulating tumor DNA (ctDNA), and telomere length.^[92] Biomarkers present in saliva for detecting diseases are listed in Table 5. DNA methylation occurs when a methyl group is added to the cytosine dinucleotide, leading to an epigenetic modification.^[93] It has been studied in saliva in

Table 5. Biologically significant markers and their concentrations in saliva.

Biomarker	Concentration	Disease	Refs.
Cotinine	1–25 ng mL ⁻¹	Smoking	[95]
Pepsin	4–500 ng mL ⁻¹	reflux-related disorders	[107a]
Amylase	2–12 U mL ⁻¹	Obesity and oral cancer	[119]
IgA	0.19 mg mL ⁻¹	Respiratory infection	[108]
IgG	0.014 mg mL ⁻¹	human cytomegalovirus	[108]
MMP-8	2.5–300 ng mL ⁻¹	inflammatory diseases, oral cancer	[120]
CRP	From 500pg to 50 µg mL ⁻¹	Pneumonia and tuberculosis	[121]
Cortisol	From 1.0 fg mL ⁻¹ to 10000 pg mL ⁻¹	Stress and Parkinson's disease	[114b]
Oxytocin	1.75–220 pg mL ⁻¹	depression and anxiety	[122]
Glucose	0.03–10 mM	Diabetes mellitus	[118a]

cancer, psychiatry, environmental, and lifestyle diseases through metabolomic analysis.^[94] One of the most alarming lifestyle risk factors is smoking, as it represents a major public health problem and has serious implications for health systems. For these reasons, a rapid and sensitive approach to identifying early smokers could be a powerful resource, especially for monitoring younger generations.

Assessing DNA methylation status using ddPCR analysis in salivary DNA samples and correlating these results with cotinine, an important biomarker of nicotine, may be an efficient tool for assessing smoking status in adolescents.^[95] The methylation of the cytosine phospho guanine (CpG) dinucleotide pair in gene cg05575921 of the aryl hydrocarbon receptor repressor is a precise marker for smoking.^[96]

Moreover, saliva cells of smokers with chronic periodontitis display a methylated SOCS1 gene promoter, whereas saliva cells of nonsmokers do not show this methylation pattern.^[97] Moreover, abuse of opioids and cannabinoids can also be detected not only by people monitoring their use but also by directly quantifying the impact of medical cannabis treatments. In total, 65 potential pharmacodynamic biomarkers sensitive to cannabis were identified using mass spectrometry analysis in patients suffering from autism spectrum disorder. The most significant biomarkers used are N-acetylaspartic acid, spermine, and dehydroisoandrosterone 3-sulfate.^[98] DNA methylation analyzed in saliva samples is also a valuable resource for screening tests and diagnosis of several other diseases, from celiac disease.^[99] to monitoring borderline personality disorder.^[100] and obesity.^[101] Telomere length analysis shows important applications in forensic science for assessing sex and age in cigarette samples.^[102] Nevertheless, sampling saliva rather than blood results in lower precision and longer telomere lengths.^[103]

Currently, the main concern regarding this class of biomarkers is the presence of both human and microbial DNA in the oral cavity. Therefore, the presence of infection must be carefully assessed before testing. The presence and concentration of microorganisms show strong correlations with some chronic diseases, and their variations may reflect an individual's health and disease status. The ability to perform analysis in real-time is an

effective solution for early warning of disease risk and prediction of treatment effects (Figure 5).^[104]

Saliva contains more than 3000 different proteins with a wide range of molecular weights that support health and can also be used as biomarkers for screening and diagnosis.^[105] Salivary enzymes include salivary amylase, lingual lipase, lysozyme, carbonic anhydrase, phosphatase, maltase, carbonic anhydrase, peroxidases, and kallikrein. They are commonly used for food digestion, as an antimicrobial agent, and for energy production. However, their use as a biomarker has also been well-studied in cardiovascular cancer, oral cancer, and Alzheimer's disease monitoring.^[106] Among them, the most studied enzymes are pepsin and amylase.^[107]

Immunoglobulins, including immunoglobulin A (IgA) and immunoglobulin G (IgG), are important to protect oral immunity through their antimicrobial activity. IgA and IgG are the most common antibodies and prevent bacteria from adhering to the surface of teeth. They can be detected in both plasma and saliva. However, the concentrations of IgG and IgA in plasma are approximately 12.5 and 2.2 mg mL⁻¹, and in saliva – 0.014 and 0.19 mg mL⁻¹, respectively. Therefore, the monitoring of IgG and IgA in saliva is limited.^[108] However, salivary IgA levels correlate with the risk of upper respiratory tract infections, and low levels may increase their frequency and duration. Higher levels can also be used to prevent SARS-COV-2 infection.^[109] IgA is also a biomarker for assessing alcohol dependence, along with other salivary glycoproteins such as α -amylase, clusterin, and haptoglobin.^[110]

Alterations in protein glycosylation have been found in many diseases, including cancer, influenza A virus, COVID-19 spike glycoprotein, and cardiovascular and neurodegenerative diseases. Aberrant glycosylation occurs during tumor genesis and evolution, hence tumor-specific glycosylation is commonly used as a biomarker.^[111]

Fifteen different lectins with strong effects on salivary glycoproteins have been proposed as biomarkers for early diagnosis of breast cancer by replacing biopsies.^[112] C-reactive protein (CRP) is an inflammatory biomarker for detecting some infectious diseases such as pneumonia and tuberculosis, as well as non-infectious diseases such as tumors or immune diseases.^[113]

In terms of hormone detection, cortisol concentration is an important indicator.^[114] Implementing point-of-care diagnostics using non-invasive ECBSs.^[114b] to replace traditional procedures such as enzyme-linked immunosorbent assay.^[115] or liquid chromatography-tandem mass spectroscopy.^[116] can be an efficient solution as these immunosensors exhibit excellent dynamic range and detection limit.^[117] Detection of salivary glucose can also be a reliable source of diagnosis for diabetes. A significant correlation exists between blood glucose levels determined through enzymes and saliva in diabetic patients.^[118] However, salivary glucose concentration may vary depending on the sampling process and storage conditions. For example, glucose levels in saliva continued to decrease with increasing stimulation levels and fluctuated throughout the day due to the circadian rhythm influence on the human body. Therefore, taking samples for analysis early in the morning is recommended.^[118a]

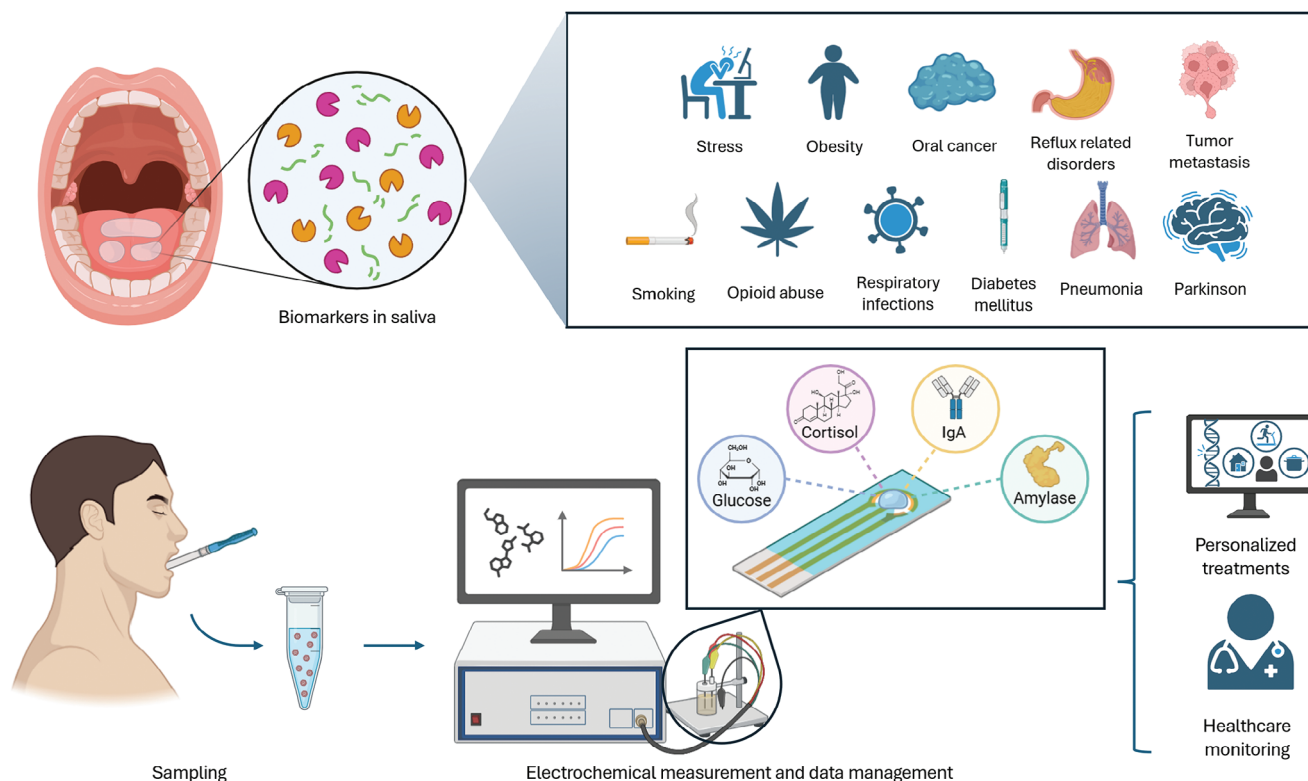


Figure 5. Conceptual representation of the ECBS system for biomarker detection in saliva. Biomarkers present in saliva samples are used to identify various pathologies or conditions of an individual. Once sampled, the saliva sample is analyzed using electrochemical measurements to detect the presence and concentration of target biomarkers. Once processed, this data can be used to identify pathologies, select personalized therapy, monitor human health status, and provide support to medical professionals. Created with BioRender.com.

2.3.2. Detection of Biomarkers in Saliva

The development of self-powered ECBSs for detecting biomarkers in saliva is a new and emerging field of research that has seen a significant increase in scientific results in recent years. The parameters of ECBSs for saliva monitoring are reported in Table 6. For example, Bolella et al. developed an innovative approach where commercial carbon-based screen-printed electrodes were functionalized with Au NPs to increase their active surface area.^[13c] In addition, *Chorinascus thermophilus* (CrCDH) and *Trametes hirsuta* laccase (ThLac) were used for the functionalization of the anode and cathode, respectively. Here, glucose detection was performed in a biofuel cell working by direct electron transfer. In this case, the electron transfer from the enzyme to the electrode does not involve redox species, which is beneficial.^[123] Experiments were carried out in a phosphate-buffered glucose solution with a glucose concentration of 100 μM , which is the maximum physiological glucose concentration in human saliva. The output power density was 1.57 $\mu\text{W cm}^{-2}$ at a V_{oc} of 0.58 V. When the electrodes were tested using real saliva, where the glucose concentration was lower compared to the synthetic solution (between 30 and 100 μM), the power density decreased to about 1.10 $\mu\text{W cm}^{-2}$ at a V_{oc} of 0.41 V. Thus, the ECBS system exhibited lower power output density when operating with real fluid. In terms of stability, the proposed solution guarantees optimal performance in the first hours of operation with a sharp drop (up to 50%) at 8 h. The output power

density was increased by combining two electrochemical cells in series (Figure 6a–d) using screen-printed electrodes (SPEs).^[43] The bioanodes were initially coated with poly-methylene blue followed by immobilization of flavin-dependent glucose dehydrogenases (FADGDH) from *Aspergillus niger* on the surface of the electrodes. Unlike GOx, FADGDH can oxidize glucose to gluconic acid without producing O_2 and H_2O_2 , thereby providing an efficient function of the enzymatic fuel cell. The biocathodes were functionalized with bilirubin oxidase, which works effectively in the normal pH range of saliva (6.2–7.6). The proposed double-cell system was tested with saliva samples ranging from 30 to 100 μM , achieving a power output of 1.4 $\mu\text{W cm}^{-2}$. This value is slightly higher than the power output value obtained using the single-cell system with SPE, which can be attributed to the low glucose concentration in saliva and the presence of interferometers.^[43] Using FADHDG instead of the basic GOx improved the stability of the device over time (half-life >24 h) due to less susceptibility to the harmful effects of molecular oxygen.

The energy level mismatch between enzymes and electrodes affects the output power density of the ECBS.^[128] Polymeric materials, in particular n-type polymers, can be used to overcome this issue. Unlike p-type polymer materials, n-types possess electron transfer properties owing to the presence of ethylene glycol in polymeric backbones, which increases the electron coupling between them and enzymes. This is a significant factor that facilitates the reaction of electrodes with an analyte, such as glucose, without the contribution of molecular oxygen, which

promotes the reduction of dioxygen. Naftalene dicarboximide and bithiophene copolymer (NDI-T2) were employed to fabricate a miniature self-powered glucose ECBS based on an enzymatic fuel cell power unit that drives an OECT as the sensing component. The OECT uses NDI-T2 polymer deposited on the Au gate electrode and channel of the transistor. The GOx enzyme was immobilized on the polymer gate film. This setup exhibited a sensing response over a wide range of glucose concentrations (10 nM–20 mM) in the electrolyte solution with a LOD of 10 nM, which is in line with other gate-functionalized electrochemical transistors.^[129] Here, the power unit contains an enzymatic fuel cell, the anode electrode of which is made based on NDI-T2, and the cathode is a p-type copolymer of ethylenedioxythiophene (EDOT) and hydroxymethyl ethylenedioxythiophene (EDOTH) capable of reducing molecular oxygen. Glucose in saliva was oxidized by GOx, producing electrons at the anode, which then flow to the cathode reducing oxygen and generating power from glucose and oxygen. The generated power density was $1.5 \mu\text{W cm}^{-2}$ at a glucose level of 100 μM , which is similar to the values achieved by other approaches reported in Table 6 and equal to the value obtained by the sensing system with double SPEs.^[123] Meanwhile, the generated power was enough to supply small electronic components such as light-emitted diodes (LEDs) or OECT. In addition, this approach enables stable functionalities over time. Using a protective polymeric layer (Nafion) on p-type polymers and membranes to divide the two electrodes enhanced the stability of the device for up to 30 days (half-life).^[124] Enzyme-based electrodes can be used in fabricating ECBS on a printed circuit board (PCB) to detect glucose in saliva. For example, highly porous Au electrodes with large surface areas were used as both bioanode and biocathode.^[125] The bioanode was modified with an osmium redox polymer, which acted as a charge transfer mediator, onto which the GOx enzyme was immobilized.

The biocathode was functionalized with bilirubin oxidase, followed by the addition of a blocking agent (StartingBlock) to prevent glucose oxidation (Figure 6a). Then, the self-powered device was tested using a buffer solution containing 1 mM glucose and artificial saliva. In the first case, an output power density of $9.6 \mu\text{W cm}^{-2}$ was achieved, and it was varied as a function of glucose concentration in the buffer. It exhibited a good sensitivity ($14.13 \mu\text{A cm}^{-2} \text{mM}^{-1}$) within the physiological range of 50 μM to 1 mM. As a proof-of-concept, the device was further tested using saliva and showed better sensitivity due to the higher conductivity of saliva ($21.5 \mu\text{A cm}^{-2} \text{mM}^{-1}$ up to 2 mM). Nevertheless, the device exhibited stable functionalities for 7 days.

Although clinical studies have identified a wide range of salivary biomarkers (Table 5), research on self-powered ECBSs has been performed mainly to detect glucose in saliva (Table 6). Meanwhile, the number of studies on self-powered ECBSs for saliva analysis is limited. Research findings indicate that enzymes are primarily used to provide selective detection of analytes in saliva. Additionally, the output power density of self-powered ECBSs using artificial saliva may be reduced when tested in real liquid. Unfortunately, there is no information about the LOD of these devices. However, the stability of these sensing systems has been tested and the results confirm their promise for future applications. Thus, further research is needed to prepare appropriate electrode materials and develop efficient electro-

chemical systems to detect other salivary biomarkers and expand the application of ECBSs.

3. Summary and Outlook

The sharply growing interest in developing self-powered ECBSs for health monitoring is evident from research conducted over the past few years. Blood analysis in the search for bioanalytes presents a challenge due to its complexity, although such body fluid is overloaded with numerous biomarkers for diagnostic purposes. Nevertheless, the abundance of metabolites that react to enzymes at very high concentrations makes blood the benchmark for self-powered biofuel cells that use enzymes to generate significant power output. Even if power generation is affected by several factors influencing the durability and stability of the supplied power, such as diffusion effects at the anode rather than the non-ideal reversibility of most available enzymatic reactions, the exploitation of biometrics over-rich in metabolites is promising for developing biosensors that can simultaneously detect an analyte and use it to generate a power source that could allow devices to operate autonomously in implantable devices.

Clinical trials show that sweat contains a wide range of biomarkers that reflect human health. Their identification and quantification provide important information about diseases and health conditions, including depression. It has been shown that there is a correlation between blood and sweat biomarkers. Therefore, high-performance BECSs for sweat monitoring can become versatile tools for non-invasive health analysis. Unlike blood sensors, electrochemical sensor systems for sweat and saliva monitoring are non-invasive. The concentration of some biomarkers in sweat is very low, and therefore particular attention should be paid to the fabrication of highly sensitive electrode materials. In this regard, the preparation of complex composite nanostructures with large surface areas where the synergy effect is considered is a very promising way to improve the electrical properties and sensitivity of ECBSs. Functionalization of electrodes with enzymes and aptamers has a crucial effect on the selective detection of specific analytes. Furthermore, nanomaterials with different morphologies improve the immobilization of enzymes. However, enzymes and aptamers can also influence charge transfer. Thus, the effect of their concentration on sensor functionality and energy production in an electrochemical system should be carefully investigated.

The use of ion-selective membranes is another effective strategy for binding specific ions. The application of compensation electrodes by isolating them with membranes has proven an efficient method for developing enzyme-free ECBSs, which may also extend the lifetime of the device. Obtaining the required amount of sweat for accurate determination of analytes is achieved after a few minutes of physical activity. Developing and integrating small-size heating elements in ECBS systems that can warm localized areas of the body and stimulate sweating can be very useful to overcome the above-mentioned issue. Biofuel cells, hydroelectric generators, and TEGs have been used to operate ECBSs. The experimental findings indicate that the amount of sweat and the ambient temperature affect the power output. Integration of miniature solar cells and rechargeable batteries into monitoring systems has been proposed to ensure their stable functionality.

Table 6. Parameters of ECBs for the detection of biomarkers in saliva.

Anode material	Cathode material	Biomarker/Biofluid	Concentration/detection range [mM]	Output	Detection method	Stability	Refs.
Graphene/AuNPs /cellobiose dehydrogenase from <i>Chorinascus Thermophilus</i> (CrCDH)	Graphite/AuNPS/ <i>Trameters</i> <i>Hirsuta</i> laccase (ThLac)	Glucose/ Saliva	0.03–0.1	Power 1.10 $\mu\text{W cm}^{-2}$	Dependence between analyte concentration and power density	Half-life >8 h	[13c]
poly-methylene blue/ FAD-Glucose dehydrogenase (FADGGDH) from <i>Aspergillus niger</i>	Bilirubin oxidase	Glucose/ Saliva	0.03–0.1	Power 1.4 $\mu\text{W cm}^{-2}$	Dependence between analyte concentration and power density	Half-life >24 h	[43]
Au/NDI-T2/COx	copolymer of ethylenedioxythiophene (EDOT) and hydroxymethyl ethylenedioxythiophene (EDOTH).	Glucose /Saliva	0.01–10	Power 1.5 $\mu\text{W cm}^{-2}$	Electrical measurement using OECT	30 d	[124]
hPG/[Os(2,2'- bipyridine) ₂ (polyvinylimidazole) ₁₀ Cl]Cl (OsPVI)/COx	hPG/bilirubin oxidase/ StartingBlock	Glucose/ Artificial Saliva	0.05–2	Current 21.5 $\mu\text{A cm}^{-2}$ mM^{-1}	Dependence between analyte concentration and power density	7 d	[125]
Graphite electrode modified with pyranose dehydrogenase immobilized with [Os(4,4'-dimethyl-2,2'- bipyridine) ₂ (poly(vinylimidazole)) ₁₀ Cl] ⁺ and carbon nanotube	Gold electrode/ <i>Myrothecium</i> <i>verrucaria</i> (BOX) adsorbed on gold nanoparticles (AuNPs)	Glucose/ Saliva	NA	Power 6 $\mu\text{W cm}^{-2}$	Linear sweep voltammetry	12 h	[126]
Gold electrode/AuNPS/CDH	Gold electrode/AuNPS/Box	Glucose/ Saliva	5 mM	Power 2.5 $\mu\text{W cm}^{-2}$	Dependence between analyte concentration and power density	NA	[127]

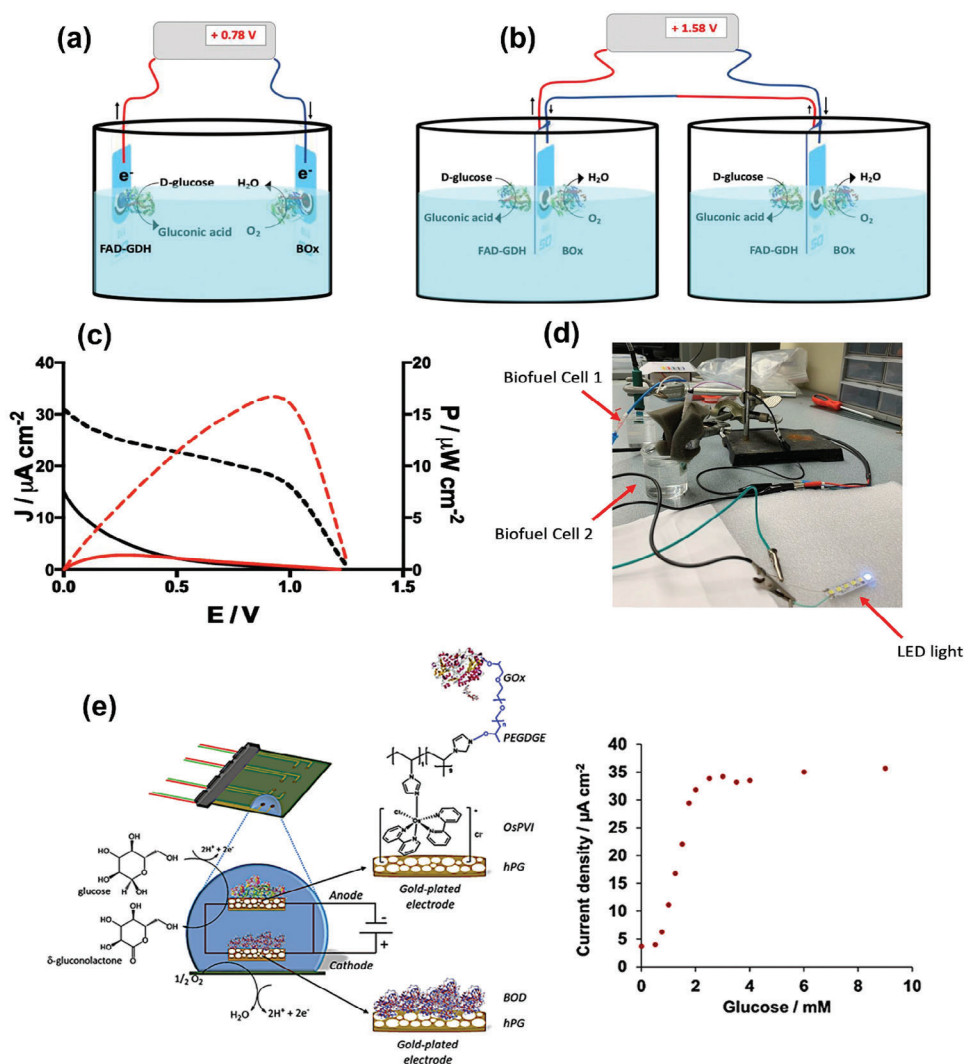


Figure 6. Schematic representation of the different EFCs assembling procedures: a) 2 normal SPEs in one electrochemical cell, one bioanode (SPE-MWCNTs/pMB25/FADGDH/PVA-SbQ) and one biocathode (SPE-MWCNTs/2-ANT/BOx); b) 2 double-sided SPEs connected in series, each one comprising both bioanode and biocathode. c) Polarization curves recorded for double-sided EFCs connected in series (SPE-MWCNTs/pMB25/FADGDH/PVA-SbQ | SPE-MWCNTs/2-ANT/BOx || SPE-MWCNTs/pMB25/FADGDH/PVA-SbQ | SPE-MWCNTs/2-ANT/BOx) in (solid black and red curves) human saliva and (dashed black and red curves) artificial human serum. The plots were obtained from linear sweep voltammetry at 1 mV s^{-1} from the OCV to 0 V. d) Double-sided EFCs connected in series operating in human saliva to power an LED light. Reproduced with permission.^[43] Copyright 2020, Elsevier. e) A schematic illustrating the operating principle of an enzymatic fuel cell fabricated on a printed circuit board. The anodic is a highly porous Au film coated with the redox polymer osmium coupled to the GOx enzyme, and the cathode is a highly porous Au film coated with bilirubin oxidase. Glucose present in saliva reacts with GOx, generating electrons that flow from the anode to the cathode, where molecular oxygen is reduced in water.^[125]

Saliva is a crucial biofluid for the early detection and prevention of diseases. Its value as a diagnostic tool is still under exploration and depends on its composition. This biofluid contains a rich set of biomarkers, metabolites, and proteins, the concentrations of which serve as indicators of various diseases such as diabetes and ischemia, among others. Therefore, saliva has been chosen as one of the benchmark biofluids used in biosensing. Self-powered ECBSs developed for salivary biomarker detection are based on immobilized enzymes. However, the proposed methods did not lead to a significant improvement in energy performance. Herein, the power output is strongly influenced by factors such as the low concentration of analyte in saliva and the

number of interferometers. The energy level mismatch between enzymes and electrodes is another factor that affects the output power density of the sensing system. Research findings suggest that preparing n-type polymers can improve the reaction of electrodes with an analyte due to their superior charge transfer properties.

Various approaches have been developed to enhance the efficiency of enzymatic fuel cells in terms of output power and long-term stability. Addressing these issues requires intensive research, including selecting the optimal redox mediator polymer to enhance enzyme/electrode interaction. In terms of long-term stability, recently proposed approaches have extended the lifetime

of enzymatic fuel cells, which are typically compromised by enzymatic degradation and instability of electrode coating layers. Strategies such as using membranes between the anode and cathode electrodes, using polymers to mitigate oxygen exposure at the anode, and applying protective layers effectively extended the life of these devices to 30 days. The use of enzymatic fuel cell systems in the field of sensors has opened the way to numerous new possibilities, especially in device miniaturization. This advancement eliminates the need for external power supplies and facilitates the transition from macroscale to microscale. Moreover, using biological fluid as an analytical medium and energy source represents a significant breakthrough, overcoming several limitations that have long hampered the production of biosensors. However, it is worth mentioning that these devices are still in their infancy. They require further improvement to operate reliably over long periods without degradation.

Thus, from the clinical research perspective, biofluids such as blood, sweat, and saliva contain a wide range of critical biomarkers that can be identified and measured using self-powered ECBSs. These devices have been intensively studied for monitoring glucose in biofluids. Most of them are enzymatic electrochemical systems providing opportunities for selective detection of glucose. Furthermore, only a few research works were performed on developing enzyme-free ECBS systems employing ion-selective membranes and semiconductor nanomaterials with unique chemical and physical properties. Unfortunately, many biomarkers present in biofluids have not yet been investigated in developing ECBSs, which is another challenge in expanding the application of self-powered ECBSs.

If the above-mentioned obstacles are overcome, self-powered ECBSs have the potential to become advanced technological tools for real-time diagnosis of health and disease. Preparing new functional nanocomposites for electrode fabrication and proposing new strategies for the efficient design of power units are key directions to advance the field of self-powered ECBSs and revolutionize the world of health monitoring systems. Thus, further research studies and development are needed to address the challenges in this area and realize the full potential of ECBSs in blood, sweat, and saliva testing.

Acknowledgements

This work was carried out within the framework of the project RAISE – Robotics and AI for Socio-economic Empowerment” and has been supported by the European Union – NextGenerationEU.

Open access publishing facilitated by Consiglio Nazionale delle Ricerche, as part of the Wiley - CRUI-CARE agreement.

Conflict of Interest

The authors declare no conflict of interest.

Keywords

biomarkers, electrochemical biosensors, monitoring of blood, monitoring of diseases, monitoring of saliva, monitoring of sweat, self-powered biosensors

Received: March 8, 2024
Revised: July 12, 2024
Published online: July 23, 2024

- [1] a) E. R. Kim, C. Joe, R. J. Mitchell, M. B. Gu, *Trends Biotechnol.* **2023**, *41*, 374; b) P. K. Bairagi, P. Rajbanshi, P. Khare, *Adv. Nanomater. Point Care Diagnos. Ther.* **2022**, 275; c) M. Agrawal, E. Prathyusha, H. Ahmed, S. K. Dubey, P. Kesharwani, G. Singhvi, V. G. M. Naidu, A. Alexander, *Neurochem. Int.* **2021**, *145*, 105008; d) A. Shiohara, M. Wojnilowicz, Q. Lyu, Y. Pei, C. D. Easton, Y. Chen, J. F. White, A. McAuley, B. Prieto-Simon, H. Thissen, N. H. Voelcker, *Small* **2023**, *19*, 2205281.
- [2] a) S. Kumari, M. Islam, A. Gupta, *Biomed. Microdevices* **2023**, *25*, 17; b) R. Qureshi, M. Irfan, H. Ali, A. Khan, A. S. Nittala, S. Ali, A. Shah, T. M. Gondal, F. Sadak, Z. Shah, M. U. Hadi, S. Khan, Q. Al-Tashi, J. Wu, A. Bermak, T. Alam, *IEEE Access* **2023**, *11*, 61600; c) K. Nityakalyani, M. C. Jobin Christ, *Mater. Sci. Semicond. Process.* **2023**, *167*, 107797.
- [3] a) E. Katz, A. F. Bückmann, I. Willner, *J. Am. Chem. Soc.* **2001**, *123*, 10752; b) R. Khan, S. Andreescu, *Biosens. Bioelectron.* **2024**, *248*, 115975; c) D. Gentili, P. D'Angelo, F. Militano, R. Mazzei, T. Poerio, M. Bruciale, G. Tarabella, S. Bonetti, S. L. Marasso, M. Cocuzza, L. Giorno, S. Iannotta, M. Cavallini, *J. Mater. Chem.* **2018**, *6*, 5400.
- [4] a) N. Apushkinskaya, E. V. Zolotukhina, E. V. Butyrskaya, Y. E. Silina, *Comput. Struct. Biotechnol. J.* **2022**, *20*, 3824; b) H. Yang, Q. Dong, D. Xu, X. Feng, P. He, W. Song, H. Zhou, *Anal. Chim. Acta.* **2023**, *1283*, 341978; c) C. Peruzzi, S. Battistoni, D. Montesarchio, M. Cocuzza, S. L. Marasso, A. Verna, L. Pasquardini, R. Verucchi, L. Aversa, V. Erokhin, P. D'Angelo, S. Iannotta, *Sci. Rep.* **2021**, *11*, 9380.
- [5] a) F. M. Gharaghani, S. Mostafapour, B. Hemmateenejad, *Biosensors* **2023**, *13*, 705; b) S. Verma, C. M. Pandey, D. Kumar, *Appl. Organomet. Chem.* **2024**, *38*, e7325.
- [6] X. Sun, H. Zhang, L. Huang, S. Hao, J. Zhai, S. Dong, *Biosens. Bioelectron.* **2021**, *177*, 112975.
- [7] A. K. Gupta, A. V. Krasnoslobodtsev, *Nanomaterials* **2023**, *13*, 1299.
- [8] a) J. Chouler, I. Bentley, F. Vaz, A. O'Fee, P. J. Cameron, M. Di Lorenzo, *Electrochim. Acta* **2017**, *231*, 319; b) Z. Xu, B. Liu, Q. Dong, Y. Lei, Y. Li, J. Ren, J. McCutcheon, B. Li, *Bioresour. Technol.* **2015**, *197*, 244; c) M. Zhou, F. Kuralay, J. R. Windmiller, J. Wang, *Chem. Commun.* **2012**, *48*, 3815.
- [9] A. J. Bandodkar, S. P. Lee, I. Huang, W. Li, S. Wang, C. J. Su, W. J. Jeang, T. Hang, S. Mehta, N. Nyberg, P. Gutruf, J. Choi, J. Koo, J. T. Reeder, R. Tseng, R. Ghaffari, J. A. Rogers, *Nature Electron.* **2020**, *3*, 554.
- [10] S. Lin, L. Xu, A. Chi Wang, Z. L. Wang, *Nat. Commun.* **2020**, *11*, 399.
- [11] Y. Li, S. N. Lai, B. Zheng, *Sens. Actuators, B* **2018**, *259*, 871.
- [12] T. Zhao, Y. Fu, C. Sun, X. Zhao, C. Jiao, A. Du, Q. Wang, Y. Mao, B. Liu, *Biosens. Bioelectron.* **2022**, *205*, 114115.
- [13] a) S. K. Sailapu, S. Liébana, I. Merino-Jimenez, J. P. Esquivel, N. Sabaté, *Biosens. Bioelectron.* **2024**, *243*, 115708; b) J. Zhao, Y. Lin, J. Wu, H. Y. Y. Nyein, M. Bariya, L.-C. Tai, M. Chao, W. Ji, G. Zhang, Z. Fan, A. Javey, *ACS Sens.* **2019**, *4*, 1925; c) P. Bollella, G. Fusco, D. Stevar, L. Gorton, R. Ludwig, S. Ma, H. Boer, A. Koivula, C. Tortolini, G. Favero, R. Antiochia, F. Mazzei, *Sens. Actuators, B* **2018**, *256*, 921.
- [14] N. Ashton, *Anaesth. Intens. Care Med.* **2013**, *14*, 261.
- [15] J. Mathew, P. Sankar, M. Varacallo, in *Physiology, Blood Plasma*, **2024**, StatPearls Publishing LLC, Treasure Island (FL) 2024.
- [16] S. Szunerits, Q. Pagneux, Y. B. M'Barek, S. Vassal, R. Boukherroub, *Bioelectrochemistry* **2023**, *153*, 108479.
- [17] J. Sun, Y. Liu, *Micromachines* **2018**, *9*, 142.
- [18] E. D. Rosen, B. M. Spiegelman, *Nature* **2006**, *444*, 847.
- [19] a) S. L. Appleton, C. J. Seaborn, R. Visvanathan, C. L. Hill, T. K. Gill, A. W. Taylor, R. J. Adams, *Diabetes Care* **2013**, *36*, 2388; b) M. Afkarian, M. C. Sachs, B. Kestenbaum, I. B. Hirsch, K. R. Tuttle, J. Himmelfarb, I. H. de Boer, *J. Am. Soc. Nephrol.* **2013**, *24*, 302; c) Y. Cui, L. Zhang, M. Zhang, X. Yang, L. Zhang, J. Kuang, G. Zhang, Q. Liu, H. Guo, Q. Meng, *Sci. Rep.* **2017**, *7*, 11195.

- [20] T. K. Mathew, M. Zubair, P. Tadi, in *Blood Glucose Monitoring*, 2024, StatPearls Publishing LLC, Treasure Island (FL) 2024.
- [21] S. E. Allen, J. L. Holm, *J. Vet. Emerg. Critic. Care* **2008**, *18*, 123.
- [22] G. Kemp, *Am. J. Physiol.: Regul., Integr. Comp. Physiol.* **2005**, *289*, R895.
- [23] V. Narwal, R. Deswal, B. Batra, V. Kalra, R. Hooda, M. Sharma, J. S. Rana, *Steroids* **2019**, *143*, 6.
- [24] R. Kleemann, L. Verschuren, M. J. van Erk, Y. Nikolsky, N. H. P. Cnubben, E. R. Verheij, A. K. Smilde, H. F. J. Hendriks, S. Zadelaar, G. J. Smith, V. Kaznacheev, T. Nikolskaya, A. Melnikov, E. Hurt-Camejo, J. van der Greef, B. van Ommen, T. Kooistra, *Genome Biol.* **2007**, *8*, R200.
- [25] S. E. Hyman, *Curr. Biol.* **2005**, *15*, R154.
- [26] H. Juárez Olguin, D. Calderón Guzmán, E. Hernández García, G. Barragán Mejía, *Oxidat. Med. Cell. Longevity* **2016**, *2016*, 1.
- [27] a) S. D. Iversen, L. L. Iversen, *Trends Neurosci.* **2007**, *30*, 188; b) F. Foroughi, M. Rahsepar, H. Kim, *J. Electroanal. Chem.* **2018**, *827*, 34.
- [28] a) S. Black, I. Kushner, D. Samols, *J. Biol. Chem.* **2004**, *279*, 48487; b) G. M. Hirschfeld, M. B. Pepys, *QJM Int. J. Med.* **2003**, *96*, 793.
- [29] a) G. F. Weber, B. G. Chousterman, S. He, A. M. Fenn, M. Nairz, A. Anzai, T. Brenner, F. Uhle, Y. Iwamoto, C. S. Robbins, L. Noiret, S. L. Maier, T. Zönnchen, N. N. Rahbari, S. Schölch, A. Klotzsche-von Ameln, T. Chavakis, J. Weitz, S. Hofer, M. A. Weigand, M. Nahrendorf, R. Weissleder, F. K. Swirski, *Science* **2015**, *347*, 1260; b) J. W. Schrader, in *JAI* **1997**, *2* (Eds: D. Leroith, Ed., C. Bondy), 49–84.
- [30] a) S. Kang, T. Tanaka, M. Narazaki, T. Kishimoto, *Immunity* **2019**, *50*, 1007; b) T. Tanaka, T. Kishimoto, *Cancer Immunol. Res.* **2014**, *288*.
- [31] M. Tertis, P. I. Leva, D. Bogdan, M. Suciú, F. Graur, C. Cristea, *Biosens. Bioelectron.* **2019**, *137*, 123.
- [32] J. Song, D. W. Park, S. Moon, H.-J. Cho, J. H. Park, H. Seok, W. S. Choi, *BMC Infect. Dis.* **2019**, *19*, 968.
- [33] E. A. Said, I. Al-Reesi, N. Al-Shizawi, S. Jaju, M. S. Al-Balushi, C. Y. Koh, A. A. Al-Jabri, L. Jeyaseelan, *J. Med. Virol.* **2021**, *93*, 3915.
- [34] G. M. Anderson, M. T. Nakada, M. DeWitte, *Curr. Opin. Pharmacol.* **2004**, *4*, 314.
- [35] a) O. Arican, M. Aral, S. Sasmaz, P. Ciragil, *Mediators Inflammation* **2005**, *2005*, 201561; b) A. J. G. Schottelius, L. L. Moldawer, C. A. Dinarello, K. Asadullah, W. Sterry, C. K. Edwards III, *Exp. Dermatol.* **2004**, *13*, 193.
- [36] J. M. G. Artigas, M. E. Garcia, M. R. A. Faure, A. M. B. Gimeno, *Postgrad. Med. J.* **1981**, *57*, 219.
- [37] M. A. Morales, J. M. Halpern, *Bioconjugate Chem.* **2018**, *29*, 3231.
- [38] V. Preziosi, M. Barra, G. Tomaiuolo, P. D'Angelo, S. L. Marasso, A. Verna, M. Cocuzza, A. Cassinese, S. Guido, *J. Mater. Chem. B* **2022**, *10*, 87.
- [39] R. V. Olkhov, R. Parker, A. M. Shaw, *Biosens. Bioelectron.* **2012**, *36*, 1.
- [40] Y. Xue, A. S. Thalmayer, S. Zeising, G. Fischer, M. Lübke, *Sensors* **2022**, *22*, 425.
- [41] K. J. Land, D. I. Boeras, X.-S. Chen, A. R. Ramsay, R. W. Peeling, *Nat. Microbiol.* **2019**, *4*, 46.
- [42] R. A. Escalona-Villalpando, A. Sandoval-García, J. R. Espinosa L, M. G. Miranda-Silva, L. G. Arriaga, S. D. Minter, J. Ledesma-García, *J. Power Sources* **2021**, *515*, 230631.
- [43] R. Zumpano, L. Lambertini, C. Tortolini, P. Bollella, G. Favero, R. Antiochia, F. Mazzei, *J. Power Sources* **2020**, *476*, 228615.
- [44] Y. Montes-Cebrián, L. del Torno-de Román, A. Álvarez-Carulla, J. Colomer-Farrarón, S. D. Minter, N. Sabaté, P. L. Miribel-Català, J. P. Esquivel, *Biosens. Bioelectron.* **2018**, *118*, 88.
- [45] H.-S. Guan, W.-Z. Song, L.-P. Huang, Z. Liu, J. Zhang, S. Ramakrishna, Y.-Z. Long, *Nanotechnology* **2022**, *33*, 025404.
- [46] R. Escalona-Villalpando, A. Sandoval-García, J. Espinosa-Lumbreras, M. Miranda-Silva, L. Arriaga, S. D. Minter, J. Ledesma-García, *ECS Meeting Abstracts* **2022**, *MA2022*, 2188.
- [47] S.-H. Huang, W.-H. Chen, Y.-C. Lin, *Energies* **2019**, *12*, 1827.
- [48] A. N. Sekretaryova, V. Beni, M. Eriksson, A. A. Karyakin, A. P. F. Turner, M. Y. Vagin, *Anal. Chem.* **2014**, *86*, 9540.
- [49] Q. Li, Y. Xu, J. Qi, X. Zheng, S. Liu, D. Lin, L. Zhang, P. Liu, B. Li, L. Chen, *Sens. Actuators, B* **2022**, *351*, 130917.
- [50] B. A. Zaccheo, R. M. Crooks, *Anal. Chem.* **2011**, *83*, 1185.
- [51] G.-H. Jeohn, S. Serizawa, A. Iwamatsu, K. Takahashi, *J. Biol. Chem.* **1995**, *270*, 14748.
- [52] G. A. Allen, A. S. Wolberg, J. A. Oliver, M. Hoffman, H. R. Roberts, D. M. Monroe, *J. Thromb. Haemost.* **2004**, *2*, 402.
- [53] L. B. Baker, A. S. Wolfe, *Eur. J. Appl. Physiol.* **2020**, *120*, 719.
- [54] W. Ji, J. Zhu, W. Wu, N. Wang, J. Wang, J. Wu, Q. Wu, X. Wang, C. Yu, G. Wei, L. Li, F. Huo, *Research* **2021**, *2021*, 9757126.
- [55] F. Gao, C. Liu, L. Zhang, T. Liu, Z. Wang, Z. Song, H. Cai, Z. Fang, J. Chen, J. Wang, M. Han, J. Wang, K. Lin, R. Wang, M. Li, Q. Mei, X. Ma, S. Liang, G. Gou, N. Xue, *Microsyst. Nanoeng.* **2023**, *9*, 1.
- [56] a) B. Schazmann, D. Morris, C. Slater, S. Beirne, C. Fay, R. Reuveny, N. Moyna, D. Diamond, *Anal. Methods* **2010**, *2*, 342; b) P. Pirovano, M. Dorrian, A. Shinde, A. Donohoe, A. J. Brady, N. M. Moyna, G. Wallace, D. Diamond, M. McCaul, *Talanta* **2020**, *219*, 121145.
- [57] S. Emaminejad, W. Gao, E. Wu, Z. A. Davies, H. Y. Y. Nyein, S. Challa, S. P. Ryan, H. M. Fahad, K. Chen, Z. Shahpar, S. Talebi, C. Milla, A. Javey, R. W. Davis, *Proc. Natl. Acad. Sci. USA* **2017**, *114*, 4625.
- [58] a) Z. Bene, Z. Fejes, M. Macek, M. D. Amaral, I. Balogh, B. Nagy, *Clin. Chim. Acta* **2020**, *508*, 277; b) V. A. LeGrys, J. R. Yankaskas, L. M. Quittell, B. C. Marshall, P. J. Mogayzel, *J. Pediatr.* **2007**, *151*, 85; c) I. A. L. Silva, A. Duarte, F. A. L. Marson, R. Centeio, T. Dousova, K. Kunzelmann, M. D. Amaral, *Front. Physiol.* **2020**, *11*, 604580.
- [59] W. Gao, S. Emaminejad, H. Y. Y. Nyein, S. Challa, K. Chen, A. Peck, H. M. Fahad, H. Ota, H. Shiraki, D. Kiriya, D.-H. Lien, G. A. Brooks, R. W. Davis, A. Javey, *Nature* **2016**, *529*, 509.
- [60] S. L. Mathis, A. I. Pivovarova, S. M. Hicks, H. Alrefai, G. G. MacGregor, *Complement. Ther. Med.* **2020**, *51*, 102417.
- [61] C. M. Ionele, M. S. Subtirelu, B. S. Ungureanu, M. S. Serbanescu, I. Rogoveanu, *Curr. Health Sci. J.* **2022**, *48*, 311.
- [62] C. A. Prompt, P. M. Quinto, C. R. Kleeman, *Nephron* **2008**, *20*, 4.
- [63] H. Y. Y. Nyein, W. Gao, Z. Shahpar, S. Emaminejad, S. Challa, K. Chen, H. M. Fahad, L.-C. Tai, H. Ota, R. W. Davis, A. Javey, *ACS Nano* **2016**, *10*, 7216.
- [64] E. Falcone, M. Okafor, N. Vitale, L. Raibaut, A. Sour, P. Faller, *Coord. Chem. Rev.* **2021**, *433*, 213727.
- [65] a) A. Chadt, H. Al-Hasani, *Pflügers Archiv – Eur. J. Physiol.* **2020**, *472*, 1273; b) X. Qing, H. Chen, F. Zeng, K. Jia, Q. Shu, J. Wu, H. Xu, W. Lei, D. Liu, X. Wang, M. Li, D. Wang, *Adv. Fiber Mater.* **2023**, *5*, 1025.
- [66] H. Zafar, A. Channa, V. Jeoti, G. M. Stojanović, *Sensors* **2022**, *22*, 638.
- [67] P. J. Derbyshire, H. Barr, F. Davis, S. P. J. Higson, *J. Physiol. Sci.* **2012**, *62*, 429.
- [68] Z. Xia, W. Zuo, H. Li, L. Qiu, R. Mu, Q. Wang, H. Liu, H. Wang, Y. Hui, *J. Appl. Electrochem.* **2023**, *54*, 1137.
- [69] F. Alam, S. RoyChoudhury, A. H. Jalal, Y. Umasankar, S. Forouzanfar, N. Akter, S. Bhansali, N. Pala, *Biosens. Bioelectron.* **2018**, *117*, 818.
- [70] a) C. Cheng, X. Li, G. Xu, Y. Lu, S. S. Low, G. Liu, L. Zhu, C. Li, Q. Liu, *Biosens. Bioelectron.* **2021**, *172*, 112782; b) M. Jia, W. M. Chew, Y. Feinstein, P. Skeath, E. M. Sternberg, *Analyst* **2016**, *141*, 2053; c) J. Liu, Z. Tao, Y. Zhang, T. Ni, B. Liu, Z. Zhang, *Microchem. J.* **2024**, *197*, 109757.
- [71] A. S. Campbell, J. Kim, J. Wang, *Curr. Opin. Electrochem.* **2018**, *10*, 126.
- [72] N. G. Costa, J. C. Antunes, A. J. Paleo, A. M. Rocha, *Biosensors* **2022**, *12*, 252.
- [73] a) Z. Sonner, E. Wilder, J. Heikenfeld, G. Kasting, F. Beyette, D. Swaile, F. Sherman, J. Joyce, J. Hagen, N. Kelley-Loughnane, R. Naik, *Biocircuits* **2015**, *9*, 031301; b) J. Kim, I. Jeeran, S. Imani, T. N. Cho, A. Bandodkar, S. Cinti, P. P. Mercier, J. Wang, *ACS Sens.* **2016**, *1*, 1011.

- [74] L. Wang, L. Pan, X. Han, M. N. Ha, K. Li, H. Yu, Q. Zhang, Y. Li, C. Hou, H. Wang, *J. Colloid Interface Sci.* **2022**, *616*, 326.
- [75] J. I. d. O. Filho, D. C. Ferreira, M. C. Faleiros, K. N. Salama, *IEEE Sens. J.* **2023**, *23*, 24179.
- [76] L. E. McCrae, W.-T. Ting, M. M. R. Howlader, *Biosens. Bioelectron.: X* **2023**, *13*, 100288.
- [77] A. Steijlen, J. Bastemeijer, R. Nederhoff, K. Jansen, P. French, A. Bossche, *Engineer. Proceed.* **2021**, *10*, 38.
- [78] J. Moyer, D. F. Wilson, I. Wong, Bruce, R. P., *Diabetes Technol. Therapeut.* **2012**, *14*, 398.
- [79] A. Ruff, P. Pinyou, M. Nolten, F. Conzuelo, W. Schuhmann, *Chem-ElectroChem* **2017**, *4*, 890.
- [80] E. V. Karpova, E. V. Shcherbacheva, A. A. Galushin, D. V. Vokhmyanina, E. E. Karyakina, A. A. Karyakin, *Anal. Chem.* **2019**, *91*, 3778.
- [81] Y. Lu, K. Jiang, D. Chen, G. Shen, *Nano Energy* **2019**, *58*, 624.
- [82] Z. Wu, Y. Zhu, X. Ji, *J. Mater. Chem. A* **2014**, 14759.
- [83] Y. Yang, X. Wei, N. Zhang, J. Zheng, X. Chen, Q. Wen, X. Luo, C.-Y. Lee, X. Liu, X. Zhang, J. Chen, C. Tao, W. Zhang, X. Fan, *Nat. Commun.* **2021**, *12*, 4876.
- [84] S. K. Sailapu, P. Kraikaew, N. Sabaté, E. Bakker, *ACS Sens.* **2020**, *5*, 2909.
- [85] X. Hu, X. Bao, M. Zhang, S. Fang, K. Liu, J. Wang, R. Liu, S. H. Kim, R. H. Baughman, J. Ding, *Adv. Mater.* **2023**, *35*, 2303035.
- [86] X. Huangfu, Y. Guo, S. M. Mugo, Q. Zhang, *Small* **2023**, *19*, 2207134.
- [87] Y. Gai, E. Wang, M. Liu, L. Xie, Y. Bai, Y. Yang, J. Xue, X. Qu, Y. Xi, L. Li, D. Luo, Z. Li, *Small Methods* **2022**, *6*, 2200653.
- [88] C. Xiong, W. Dang, Q. Yang, Q. Zhou, M. Shen, Q. Xiong, M. An, X. Jiang, Y. Ni, X. Ji, *Adv. Sci.* **2023**, *11*, 2305962.
- [89] W. M. Edgar, *Br. Dent. J.* **1992**, *172*, 305.
- [90] S. Nishitani, S. E. Parets, B. W. Haas, A. K. Smith, *Epigenetics* **2018**, *13*, 352.
- [91] F. G. Bellagambi, T. Lomonaco, P. Salvo, F. Vivaldi, M. Hangouët, S. Ghimenti, D. Biagini, F. Di Francesco, R. Fuoco, A. Errachid, *TRAC Trends Analyt. Chem.* **2020**, *124*, 115781.
- [92] M. Song, H. Bai, P. Zhang, X. Zhou, B. Ying, *Int. J. Oral Sci.* **2023**, *15*, 2.
- [93] C. N. Flores-Fernández, D. Lin, K. Robins, C. A. O'Callaghan, *Appl. Microbiol. Biotechnol.* **2024**, *108*, 174.
- [94] E. E. Balashova, D. L. Maslov, P. G. Lokhov, *J. Personal. Med.* **2018**, *8*, 28.
- [95] K. Dawes, A. Andersen, K. Vercande, E. Papworth, W. Philibert, S. R. H. Beach, F. X. Gibbons, M. Gerrard, R. A. Philibert, *J. Child Adolescent Psychopharmacol.* **2019**, *29*, 535.
- [96] A. M. Andersen, M. V. Dogan, S. R. H. Beach, R. A. Philibert, *Genes* **2015**, *6*, 991.
- [97] C. d. J. H. Martinez, K. R. V. Villafuerte, H. R. Luchiar, J. d. O. Cruz, M. Sales, D. B. Palioto, M. R. Messori, S. L. S. Souza, M. Taba Jr., E. S. Ramos, A. B. Novaes Jr., *J. Periodontol.* **2019**, *90*, 1279.
- [98] M. Siani-Rose, S. Cox, B. Goldstein, D. Abrams, M. Taylor, I. Kurek, *Cannabis Cannabin. Res.* **2023**, 126.
- [99] N. L. Hearn, A. S. Coleman, V. Ho, C. L. Chiu, J. M. Lind, *BMC Genomics* **2019**, *20*, 163.
- [100] M. Thomas, N. Knoblich, A. Wallisch, K. Glowacz, J. Becker-Sadzio, F. Gundel, C. Brückmann, V. Nieratschker, *Clin. Epigenet.* **2018**, *10*, 109.
- [101] I. Matias, B. Gatta-Cherifi, A. Tabarin, S. Clark, T. Leste-Lasserre, G. Marsicano, P. V. Piazza, D. Cota, *PLoS One* **2012**, *7*, e42399.
- [102] M. Schellnegger, A. C. Lin, N. Hammer, L.-P. Kamolz, *Sports Med. Open* **2022**, *8*, 111.
- [103] A. T. Geronimus, J. Bound, C. Mitchell, A. Martinez-Cardoso, L. Evans, L. Hughes, L. Schneper, D. A. Notterman, *PLoS One* **2021**, *16*, 0255237.
- [104] X. Peng, L. Cheng, Y. You, C. Tang, B. Ren, Y. Li, X. Xu, X. Zhou, *Int. J. Oral Sci.* **2022**, *14*, 14.
- [105] F. M. L. Amado, R. P. Ferreira, R. Vitorino, *Clin. Biochem.* **2013**, *46*, 506.
- [106] S. P. Humphrey, R. T. Williamson, *J. Prosthet. Dentist.* **2001**, *85*, 162.
- [107] a) C.-P. Wang, C.-C. Wang, H.-C. Lien, W.-J. Lin, S.-H. Wu, K.-L. Liang, S.-A. Liu, *Laryngoscope* **2019**, *129*, 709; b) M. Kheirmand Parizi, H. Akbari, M. Malek-mohamadi, M. Kheirmand Parizi, S. Kakoei, *BMC Oral Health* **2019**, *19*, 175.
- [108] F. M. L. Amado, N. de Haan, A. Bondt, J. Murli, V. Dotz, M. Wührer, *Fronti. Immunol.* **2018**, *9*, 2436.
- [109] K. Tsukinoki, T. Yamamoto, K. Handa, M. Iwamiya, J. Saruta, S. Ino, T. Sakurai, *PLoS One* **2021**, *16*, 0249979.
- [110] N. Waszkiewicz, S. Chojnowska, A. Zalewska, K. Zwierz, A. Szulc, S. D. Szajda, *Alcohol Alcoholism* **2014**, *49*, 409.
- [111] Z. Gao, M. Xu, S. Yue, H. Shan, J. Xia, J. Jiang, S. Yang, *Curr. Res. Pharmacol. Drug Disc.* **2022**, *3*, 100079.
- [112] X. Liu, H. Yu, Y. Qiao, J. Yang, J. Shu, J. Zhang, Z. Zhang, J. He, Z. Li, *EBioMedicine* **2018**, *28*, 70.
- [113] E. B. Windgassen, L. Funtowicz, T. N. Lunsford, L. A. Harris, S. L. Mulvagh, *Postgrad. Med.* **2011**, *123*, 114.
- [114] a) H. S. Bracha, *CNS Spectrums* **2004**, *9*, 679; b) J. Liu, N. Xu, H. Men, S. Li, Y. Lu, S. S. Low, X. Li, L. Zhu, C. Cheng, G. Xu, Q. Liu, *Sensors* **2020**, *20*, 1422.
- [115] O. Thomsson, B. Ström-Holst, Y. Sjunnesson, A.-S. Bergqvist, *Acta Veterinaria Scandinavica* **2014**, *56*, 55.
- [116] H. Kataoka, E. Matsuura, K. Mitani, *J. Pharm. Biomed. Anal.* **2007**, *44*, 160.
- [117] A. Sharma, A. Wulff, A. Thomas, S. Sonkusale, *Microchim. Acta* **2024**, *191*, 103.
- [118] a) Y. Cui, H. Zhang, S. Wang, J. Lu, J. He, L. Liu, W. Liu, *Biomolecules* **2022**, *12*, 1335; b) Y. Cui, H. Zhang, J. Zhu, L. Peng, Z. Duan, T. Liu, J. Zuo, L. Xing, Z. Liao, S. Wang, W. Liu, *Appl. Sci.* **2021**, *11*, 11367.
- [119] V. Selvaraju, C. M. Venkatapoorna, J. R. Babu, T. Geetha, *Diab. Metab. Syndr. Obesity-Targets Ther.* **2020**, *13*, 1695.
- [120] C. Tortolini, V. Gigli, A. Angeloni, F. Tasca, N. T. K. Thanh, R. Antiochia, *Bioelectrochemistry* **2024**, *156*, 108590.
- [121] Q.-Q. An, X.-Z. Feng, T. Zhan, Y.-Y. Cheng, G.-C. Han, Z. Chen, H.-B. Kraatz, *Talanta* **2024**, *267*, 125158.
- [122] J. C. Caicedo Mera, M. A. Cárdenas Molano, C. C. García López, C. Acevedo Triana, J. Martínez Cotrina, *Heliyon* **2021**, *7*, e08289.
- [123] S. ul Haque, A. Nasar, N. Duteanu, S. Pandey, Inamuddin, *Fuel* **2023**, *331*, 125634.
- [124] D. Ohayon, G. Nikiforidis, A. Savva, A. Giugni, S. Wustoni, T. Palanisamy, X. Chen, I. P. Maria, E. Di Fabrizio, P. M. F. J. Costa, I. McCulloch, S. Inal, *Nat. Mater.* **2020**, *19*, 456.
- [125] C. Gonzalez-Solino, E. Bernalte, C. Bayona Royo, R. Bennett, D. Leech, M. Di Lorenzo, *ACS Appl. Mater. Interfaces* **2021**, *13*, 26704.
- [126] P. Ó Conghaile, M. Falk, D. MacAodha, M. E. Yakovleva, C. Gonaus, C. K. Peterbauer, L. Gorton, S. Shleev, D. Leech, *Anal. Chem.* **2016**, *88*, 2156.
- [127] M. Falk, Z. Blum, S. Shleev, *Electrochim. Acta* **2012**, *82*, 191.
- [128] R. A. S. Luz, A. R. Pereira, J. C. P. de Souza, F. C. P. F. Sales, F. N. Crespihlo, *ChemElectroChem* **2014**, *1*, 1751.
- [129] a) N. Gao, R. Zhou, B. Tu, T. Tao, Y. Song, Z. Cai, H. He, G. Chang, Y. Wu, Y. He, *Anal. Chim. Acta* **2023**, *1239*, 340719; b) C. Liao, M. Zhang, L. Niu, Z. Zheng, F. Yan, *J. Mater. Chem. B* **2013**, *3820*; c) C. Liao, C. Mak, M. Zhang, H. L. W. Chan, F. Yan, *Adv. Mater.* **2015**, *27*, 676.



Vardan Galstyan is a researcher at the Institute of Materials for Electronics and Magnetism, National Research Council (IMEM-CNR) of Italy. He got his Ph.D. degree in 2008 from the Yerevan State University. In 2022, V. Galstyan obtained National Scientific Habilitation as a Full Professor in the Italian higher education system. His research activities mainly deal with the synthesis of organic/inorganic nanomaterials and nanocomposites, as well as the investigation of their fundamental and functional properties for applications in gas and biosensors, energy, and biomedicine.



Ilenia D'Onofrio is currently a Ph.D. student in Material Science and Technology at the Department of Chemical, Life and Environmental Sustainability Sciences of the University of Parma, in collaboration with the Institute of Materials for Electronics and Magnetism, National Research Council (IMEM-CNR) of Italy. She received her master's degree in Genomic, Molecular, and Industrial Biotechnologies from the University of Parma. Her current research focuses on biosensing devices and the synthesis and characterization of polymer-based drug delivery systems and their applications in healthcare.



Aris Liboà graduated in food safety and food risk management at the University of Modena and Reggio Emilia (Italy). He is a Ph.D. student in Material Science and Technology at the Department of Chemical, Life, and Environmental Sustainability Sciences of the University of Parma, in collaboration with the Institute of Materials for Electronics and Magnetism, National Research Council (IMEM-CNR) of Italy. His research activity deals with the development of electrochemical biosensors and drug delivery systems for the food and feed industry.



Giuseppe De Giorgio is a Postdoctoral Researcher at the Institute of Materials for Electronics and Magnetism, National Research Council (IMEM-CNR) of Italy. In 2022, he received his Ph.D. in Biotechnology and Biosciences at the Department of Chemistry, Life Sciences and Environmental Sustainability, University of Parma. His main research interests are the synthesis of biomaterials for biomedical and sensor applications, the development of innovative drug delivery systems, the synthesis and characterization of nanoparticles and nanostructured materials, and the application of engineered materials for the treatment of human diseases.



Davide Vurro received his MSc in Science and Technologies of Materials (STM) from the University of Bari, Aldo Moro in 2016. Afterward, he received a Ph.D. degree in STM at the University of Parma in 2019. Currently, D. Vurro is a researcher at the Institute of Materials for Electronics and Magnetism, National Research Council (IMEM-CNR) of Italy. His research covers processes such as additive manufacturing techniques to develop biocompatible and sustainable biopolymer-based materials for bioelectronics and energy applications.



Luigi Rovati graduated (summa cum laude) in Electronic Engineering from the University of Pavia in 1989 and earned his Ph.D. in Electronics Engineering from the same university in 1994. Currently, he is a Full Professor of Measurement Engineering and Instrumentation at the Department of Engineering “Enzo Ferrari” at the University of Modena e Reggio Emilia (Italy). His research focuses on developing innovative sensors and measurement instruments, particularly in the biomedical field. He has received numerous awards for his contributions and has coordinated and participated in various national and international research projects.



Giuseppe Tarabella is a researcher at the CNR (IT). He received his Ph.D. in Materials Science in 2012 at the University of Parma, working in the Organic Electronics area, especially with Organic Transistors applied as biosensors. His main interests are in 1) Sensor devices for diagnostics and biosensing; 2) 3D printing for wearable and flexible electronics; 3) Electrochemical characterization and surface bio-functionalization; and 4) Unconventional Computing. Since 2022, he has been the IMEM-CNR unit coordinator of the European Project EIC, IV-Lab Pathfinder Challenge, the project's goal being the development of non-invasive sensors for the continuous monitoring of one's health state.



Pasquale D'Angelo graduated in Physics and received his Ph.D. in “Innovative Technologies for Materials, Sensor and Imaging” at the University of Naples Federico II. He devoted his post-doctoral activities to serving as a Research Fellow at the Institute for the Study of Nanostructured Materials, Bologna, Institute de Science et d'Ingénierie Supramoléculaires, Strasbourg, and Imperial College, London. Since 2012, he has worked as a researcher at the Institute of Materials for Electronics and Magnetism, National Research Council (IMEM-CNR) of Italy, where he conducts research on organic-based electronic/bioelectronic devices to realize several types of applications including biosensors, neuromorphic devices, and energy.